NATIONAL CENTER FOR EARTHQUAKE
ENGINEERING RESEARCH
State University of New York at Buffalo

(PERIMENTAL INVESTIGATION OF PRIMARY - SECONDARY SYSTEM INTERACTION

by

G.D. Manolis, G. Juhn and A.M. Reinhorn
Department of Civil Engineering
State University of New York at Buffalo
Buffalo, New York 14260

Technical Report NCEER-88-0019

May 27, 1988

This research was conducted at the State University of New York at Buffalo and was partially supported by the National Science Foundation under Grant No. ECE 86-07591.

NOTICE

This report was prepared by the State University of New York at Buffalo as a result of research sponsored by the National Center for Earthquake Engineering Research (NCEER) and the National Science Foundation. Neither NCEER, associates of NCEER, its sponsors, State University of New York at Buffalo, nor any person acting on their behalf:

a. makes any warranty, express or implied, with respect to the use of any information, apparatus, method, or process disclosed in this report or that such use may not infringe upon privately owned rights; or

b. assumes any liabilities of whatsoever kind with respect to the use of, or for damages resulting from the use of, any information, apparatus, method or process disclosed in this report.

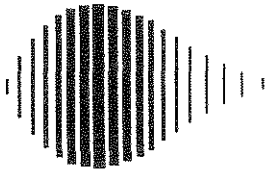

EXPERIMENTAL INVESTIGATION OF PRIMARY - SECONDARY SYSTEM INTERACTION

by

G.D. Manolis[1], G. Juhn[2] and A.M. Reinhorn[3]

May 27, 1988

Technical Report NCEER-88-0019

NCEER Contract Number 86-3022 and 87-2009

NSF Master Contract Number ECE 86-07591

1 Associate Professor, Dept. of Civil Engineering, State University of New York at Buffalo
2 Graduate Student, Dept. of Civil Engineering, State University of New York at Buffalo
3 Associate Professor, Dept. of Civil Engineering, State University of New York at Buffalo

NATIONAL CENTER FOR EARTHQUAKE ENGINEERING RESEARCH
State University of New York at Buffalo
Red Jacket Quadrangle, Buffalo, NY 14261

PREFACE

The National Center for Earthquake Engineering Research (NCEER) is devoted to the expansion of knowledge about earthquakes, the improvement of earthquake-resistant design, and the implementation of seismic hazard mitigation procedures to minimize loss of lives and property. Initially, the emphasis is on structures and lifelines of the types that would be found in zones of moderate seismicity, such as the eastern and central United States.

NCEER's research is being carried out in an integrated and coordinated manner following a structured program. The current research program comprises four main areas:

- Existing and New Structures
- Secondary and Protective Systems
- Lifeline Systems
- Disaster Research and Planning

This technical report pertains to the second program area and, more specifically, to secondary systems.

In earthquake engineering research, an area of increasing concern is the performance of secondary systems which are anchored or attached to primary structural systems. Many secondary systems perform vital functions whose failure during an earthquake could be just as catastrophic as that of the primary structure itself. The research goals in this area are to:

1. Develop greater understanding of the dynamic behavior of secondary systems in a seismic environment while realistically accounting for inherent dynamic complexities that exist in the underlying primary-secondary structural systems. These complexities include the problem of tuning, complex attachment configuration, nonproportional damping, parametric uncertainties, large number of degrees of freedom and nonlinearities in the primary structure.
2. Develop practical criteria and procedures for the analysis and design of secondary systems.
3. Investigate methods of mitigation of potential seismic damage to secondary systems through optimization or protection. The most direct route is to consider enhancing their performance through optimization in their dynamic characteristics, in their placement within a primary structure or in innovative design of their supports. From the point of view of protection, base isolation of the primary structure or the application of other passive or active protection devices can also be fruitful.

Current research in secondary systems involves activities in all three of these areas. Their interaction and interrelationships with other NCEER programs are illustrated in the accompanying figure.

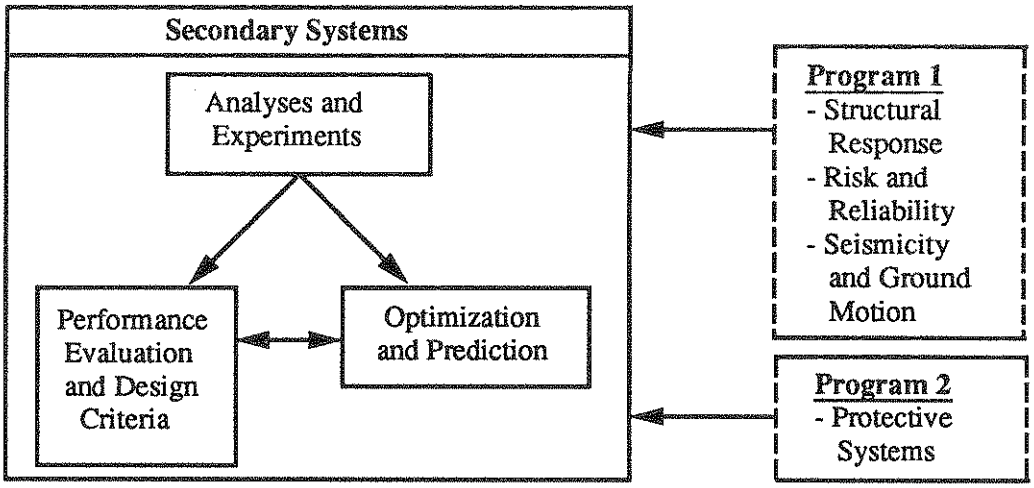

Results of an experimental investigation on the interaction between primary and secondary structural systems are presented in this report. Results were obtained for both tuned and detuned situations and for a range of primary-secondary mass ratios. This will be followed by a more comprehensive experimental program involving more realistic models.

ABSTRACT

A series of experiments were conducted on an earthquake simulator, whereby single degree-of-freedom pendulums (dampers) representing a secondary system were attached to the floor of a scaled, three story frame representing the primary structure. The dampers had mass ratios ranging from one-tenth to one-hundredth with respect to the mass of the story they were attached to. Both tuned and de-tuned cases were examined. Two types of excitations were imparted from the earthquake simulator to the frame with an attached damper, namely, white noise for identification purposes and the El Centro 1940 accelerogram. The results of these tests are grouped into transfer functions resulting from the white noise excitation and time histories resulting from the El Centro 1940 accelerogram. These results are followed by interpretations using numerical techniques developed previously for this purpose. Good correlation between the experimental evidence and the theoretical predictions is obtained, which points to that fact that interaction between primary and secondary systems does occur and can be detected.

ACKNOWLEDGEMENTS

The authors wish to thank Mr. Yen-Po Wang, a graduate student in the Civil Engineering department, and Messrs. Mark Pitman and Dan Walch, who are responsible for operating the earthquake simulator facility of the Civil Engineering department.

TABLE OF CONTENTS

LIST OF ILLUSTRATIONS

LIST OF TABLES

SECTION I

INTRODUCTION

Experimental evidence of primary-secondary system interaction in this country seems to be scant. With the exception of a series of tests conducted by Kelly (1982) in the context of base isolation of the primary structure, little else is available. In particular, Kelly (1982) placed three small vertical cantilevers of mass ratio with respect to the mass of the supporting floor of 1 to 500 on the second and fifth floors of a one-third scale, five story steel frame. The purpose of the experiment was to test the ability of three base isolation systems to reduce the response of the primary system. The cantilevers were too light to allow general conclusions to be drawn. Instead, the behavior of secondary systems was deduced from the behavior of the primary structure.

It seems likely that experimental investigations of primary-secondary system interaction, especially in the context of base isolation, have been done in Japan but this is research work done by private companies. As such, it is difficult to trace it in the open literature. As an example, Suzuki et al (1987) reported experimental work, actual observations and numerical simulations for a large electrical transformer resting on a base isolation system with sliding elements. The electrical transformer can be considered to behave as a single degree-of-freedom (DOF) secondary system resting on its base-isolated foundation. Soil-structure interaction effects become important for this type of problem.

In contrast to experimental work, there is a wealth of analytical-numerical work on secondary systems. This work ranges from older floor response spectrum approaches used in design that do not account for primary-

secondary system interaction (Kapur and Shao 1973) to newer floor response spectra that do take the interaction effect into account (Burdisso and Singh 1987).

Also, both perturbation techniques based on the fact that the secondary system is usually much lighter than the primary structure (Sackman and Kelly 1979, Der Kiureghian et al 1983) and eigensolution methodologies (Suarez and Singh 1987) where the eigenproperties of the combined system are synthesized from the eigenproperties of the separate primary and secondary systems have been developed. Other approaches include simplified component mode synthesis (Villaverde 1986), transfer functions (HoLung et al 1987), and substructuring in conjunction with time integration (Singhal et al, 1988; Manolis and Juhn 1988).

In what follows, the experiment involving secondary systems in the form of pendulums placed in a fixed base, scaled rigid frame is described. Results are obtained for two types of ground motions, a white noise accelerogram and the 1940 El Centro accelerogram. The former results are used in experimental identification of the primary-secondary system. Using this information, the substructuring techniques in the time domain developed by Manolis and Juhn (1988) are used to reproduce time histories for the 1940 El Centro accelerogram, which are subsequently compared with experimentally obtained results.

SECTION 2

DESCRIPTION OF THE EXPERIMENT

2.1 The Primary Structure

A three story, one-quarter scale rigid steel frame was used to model the primary structure. This frame was bolted to the top surface of the shaking table that is part of the earthquake simulator facility of the department of Civil Engineering of the State University of New York at Buffalo (Hwang et al, 1987). A detailed drawing of this frame is shown in Fig. 2-1. The frame has welded, moment resisting connections and behaves much like a three DOF shear building when subjected to lateral loads. Additional weights had to be added at each floor to satisfy dynamic similitude requirements. Also, the frame is braced in the transverse direction and is fixed at the base. This frame was previously used in a series of experiments on active structural control (Chung et al, 1988).

Representative properties of this frame were experimentally identified and are listed in Table 2-I. It should be noted that there is a slight variation of the stiffness of the frame from one dynamic shaking episode to another, which results in changes in the natural frequencies and damping factors on the order of one percent. To compensate for this, experimental identification using white noise as the ground motion is done prior to any shaking episode to obtain the most current values of the natural frequencies and damping factors of the frame.

2.2 The Secondary Systems

Dampers, which are vertical cantilivers fixed at the bottom with steel plates attached to the top, were fabricated and represent single DOF

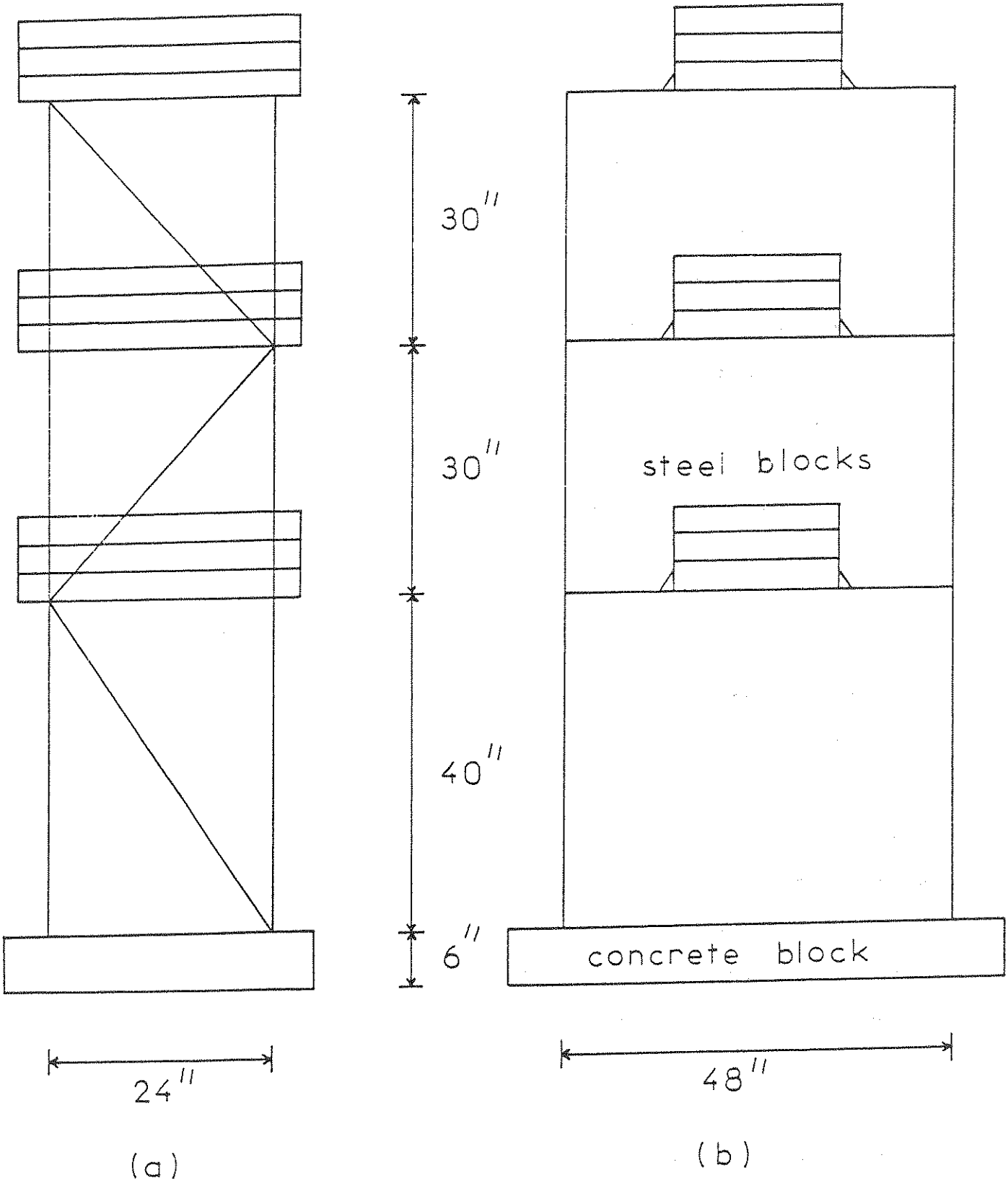

Figure 2-1 Three Story Scaled Steel Frame: (a) Side View (b) Front View

TABLE 2-I

Primary Structure Properties

M (mass matrix in lb-s^2/in.)	5.6 0 0	 5.6 0	sym. 5.6
K (stiffness matrix in lb/in.)	16,065 -9,406 2,206	 16,423 -9,152	sym. 7861
C (damping matrix in lb-s /in.)	3,093 -0.380 0.080	 3.062 -0.438	sym. 2.913
ω_n (natural frequencies in Hz)		2.25 6.84 11.43	
ζ_n (modal damping factors as %)		1.57 0.61 0.45	
ϕ (modal matrix)	0.115 0.242 0.326	0.314 0.150 -0.239	0.252 -0.302 0.155
Γ (modal participation factors)		3.83 1.26 0.59	

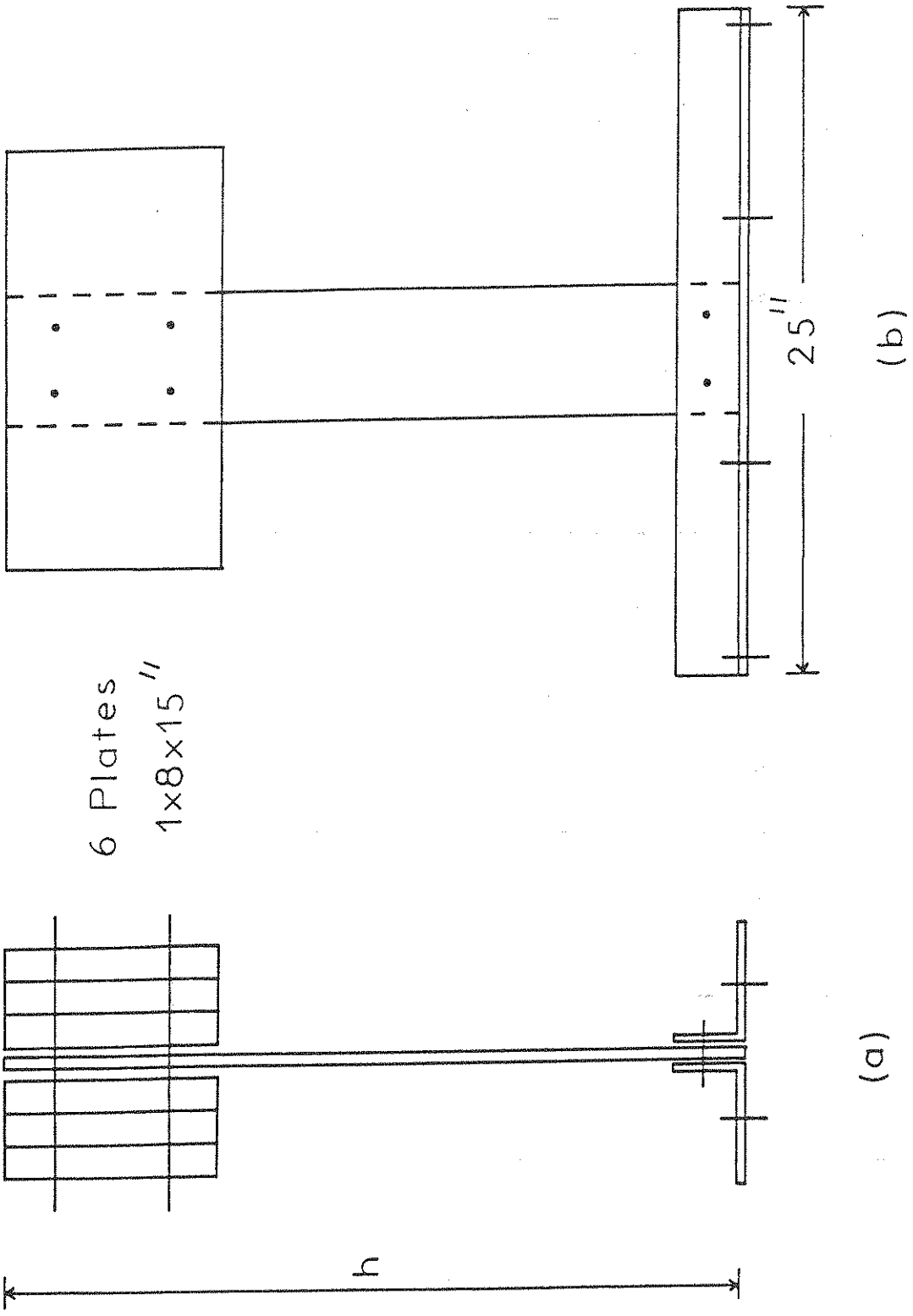

Figure 2-2 Damper B and Base Attachment System: (a) Front View (b) Side View

secondary systems. A typical such damper is shown in Fig. 2-2. Actually, a series of dampers can be generated by combining eight vertical cantilevers and twelve steel plates. Three of these cantilevers and two of the plates are pictured in Fig. 2-3. The properties of the four cases that were considered here are listed in Table 2-II. The natural frequencies and damping ratios of each damper were first determined using an impact hammer. To insure that any minor changes in the damper stiffness are accounted for, the same experimental identification process used for the frame prior to any shaking episode yielded information on the damper that was also attached to the frame.

2.3 The Coupled System

Four coupled systems resulted by fixing each of the dampers of Table 2-II to the second floor of the frame. A typical configuration is shown in Fig. 2-4. These four combinations produce two tuned cases of the damper with the first mode of the frame and two detuned cases, namely, one where the frequency of the damper is lower than that of the first frequency of the frame and one where it is higher. Also, two basic mass ratios are reproduced: one where three dampers have a mass of around 10% of the mass of floor of the frame to which they are attached, and one where one damper has a mass ratio equal to 1%. Figures 2-4 through 2-6 pictures of the combined system before it was tested. In particular, Figs. 2-4 and 2-5 are a front view and a side view of the coupled system, respectively, while Fig. 2-6 is a close-up of the second story of the frame where the damper is attached.

Each of the four coupled system combinations were subjected to two types of ground motions delivered through the shaking table: a white noise

TABLE 2-II

Secondary System Properties

Damper	BT	BU	C	E
m (mass in lb-s^2/in.)	0.362	0.414	0.543	0.065
k (stiffness in lb/in.)	89.4	72.1	721.8	3.68
c (damping in lb-s/in.)	0.114	0.109	0.396	0.016
ω (natural frequency in Hz)	2.5	2.1	5.8	1.2
ζ (damping ratio as %)	1.0	1.0	1.0	1.0

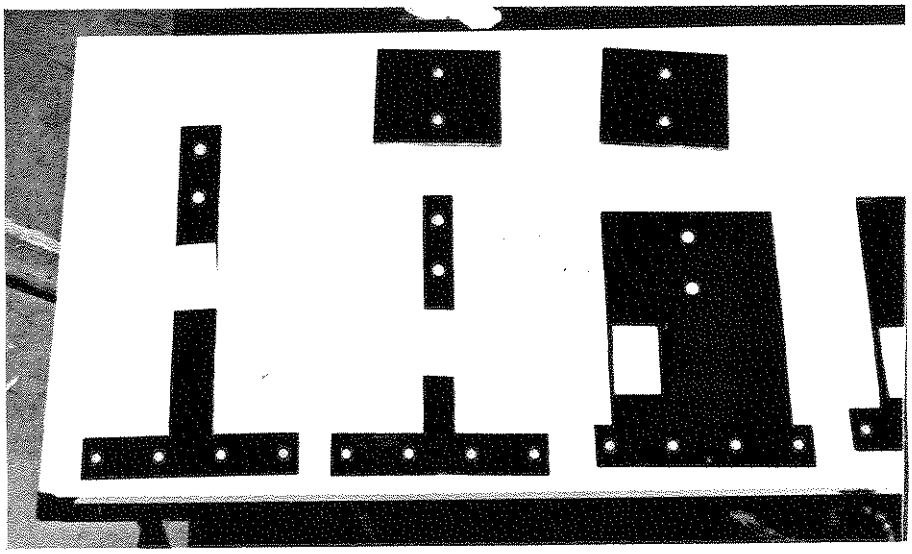

Figure 2-3 Detailed View of Unassembled Dampers E, F and G

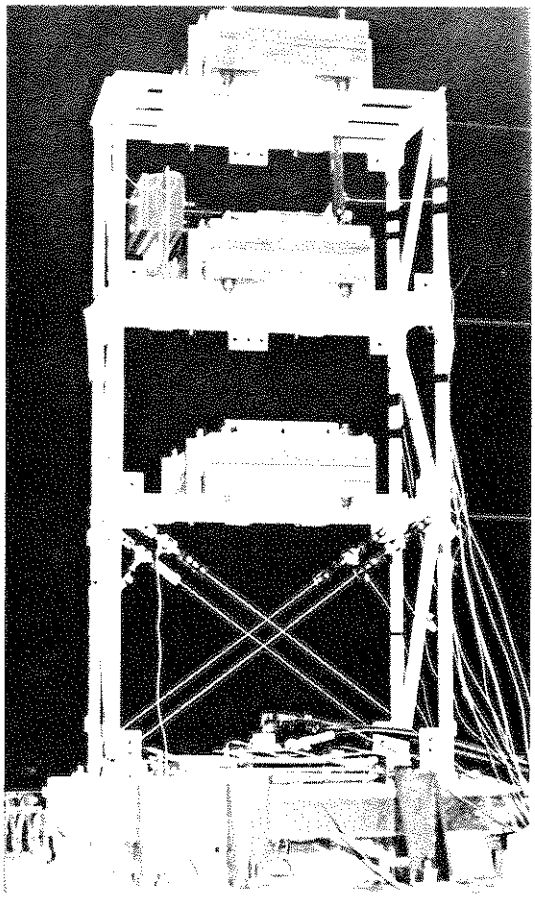

Figure 2-4 Front View of Three Story Scaled Frame with Damper B

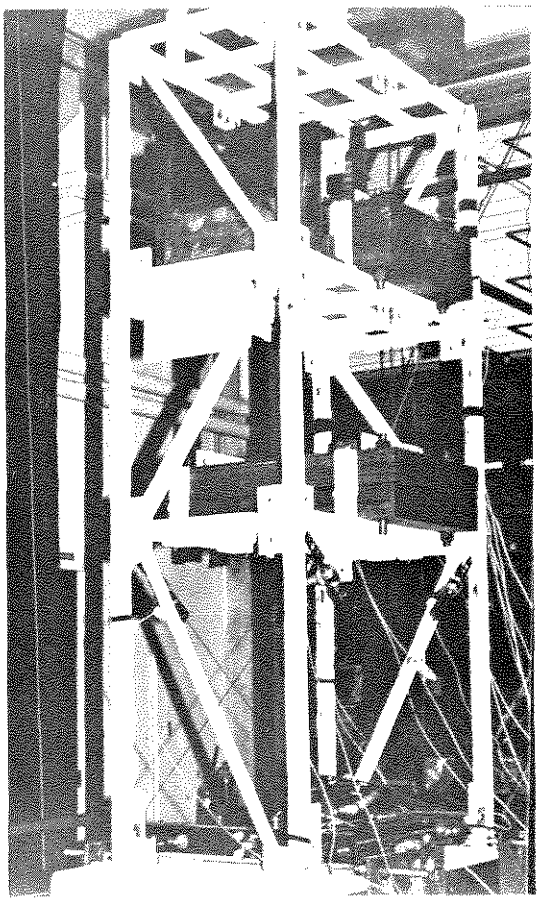

Figure 2-5 Side View of Three Story Scaled Frame With Damper D

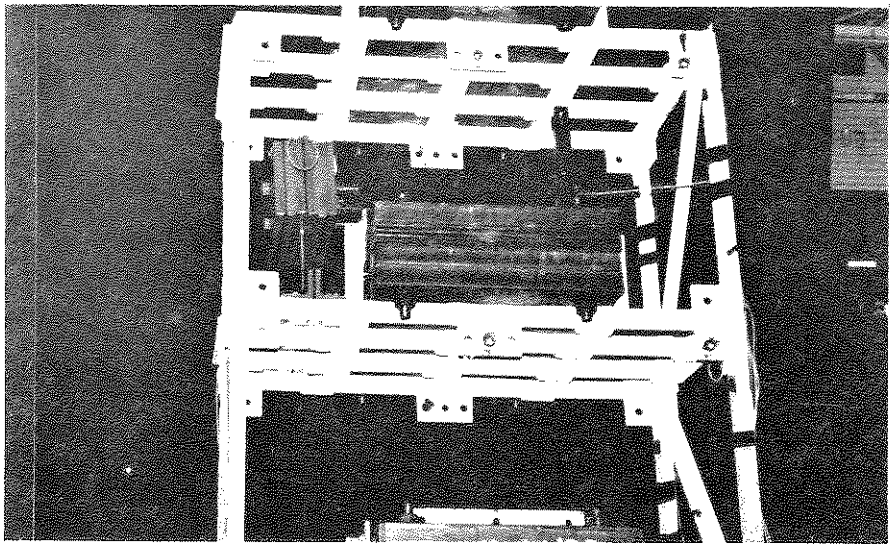

Figure 2-6 Detailed Front View of Three Story Scaled frame with Damper B

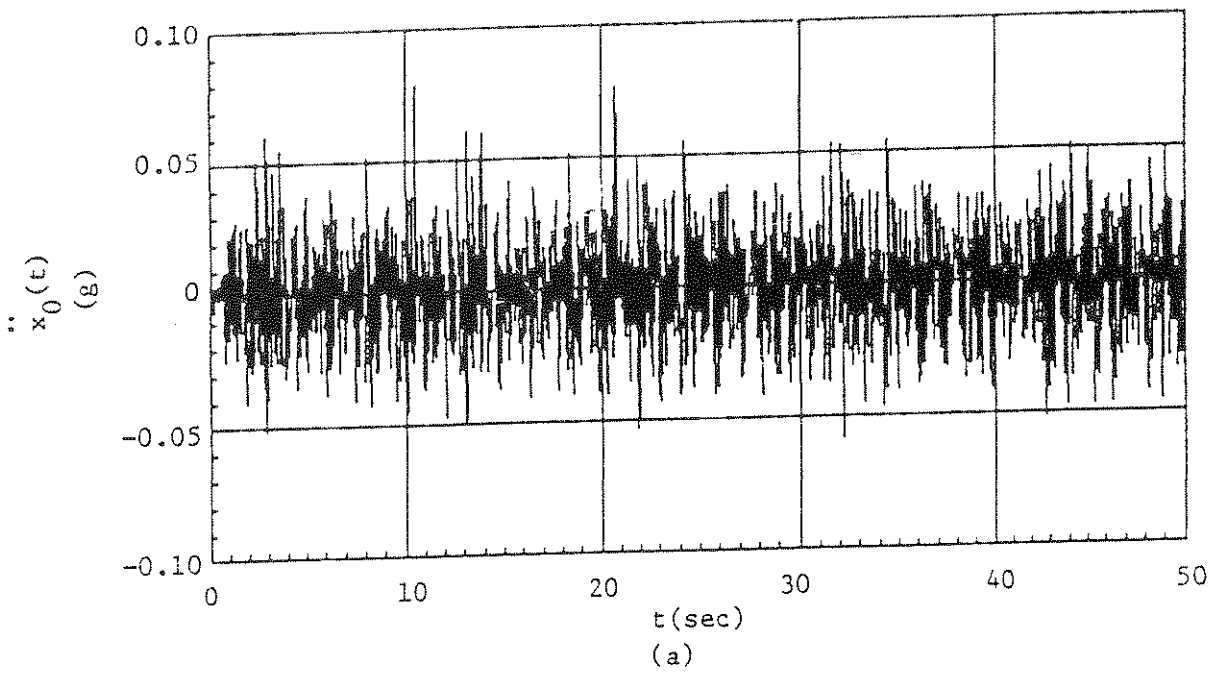

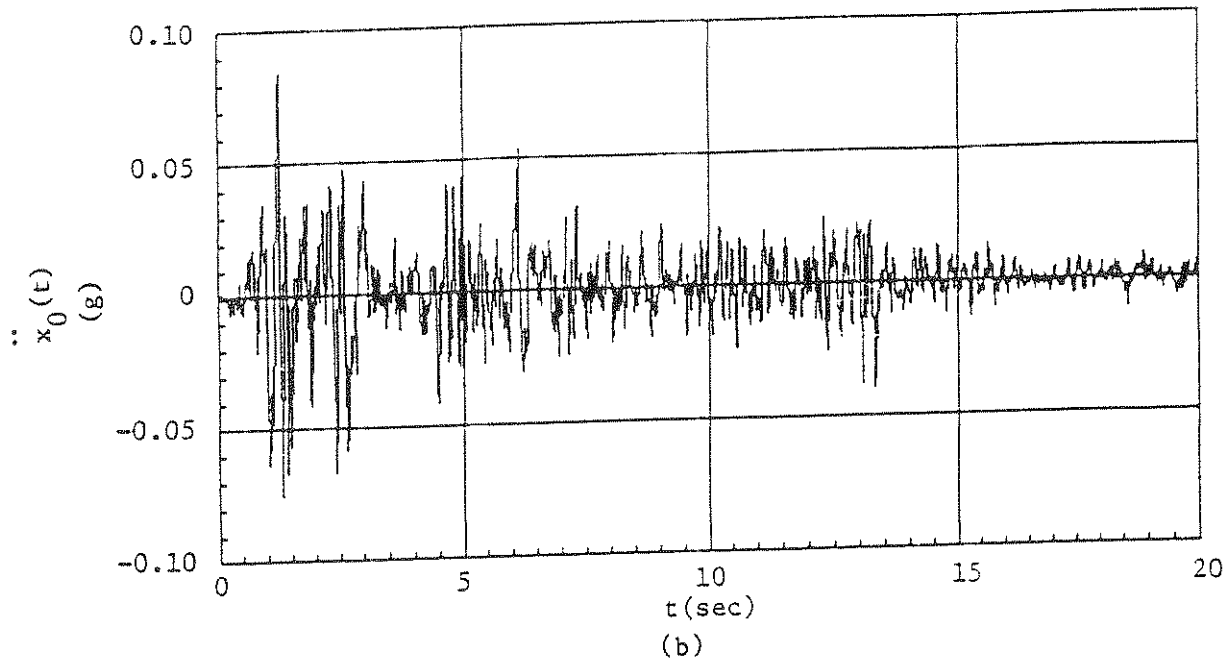

Figure 2-7 (a) White Noise and (b) El Centro 1940 Accelerograms

ground acceleration shown in Fig. 2-7(a) and the El Centro 1940 N-S accelerogram shown in Fig. 2-7(b). The two records are scaled to a maximum peak acceleration of 0.05g and 0.076g, respectively, with g being the acceleration of gravity, and have a 60s and a 30s duration, respectively. The white noise signal is banded in the 0-15 Hz frequency range. Shaking was uni-directional and along the front view, i.e., Fig. 2-4, of the frame.

2.4 Instrumentation and Data Collection

The coupled system was instrumented with Endevco type accelerometers and Temposonic type displacement transducers. As shown in Fig. 2-8, five accelerometers monitored the absolute accelerations of the base, first, second and third stories of the frame and of the damper. Also, five displacement transducers monitored the relative displacements of the base, first, second and third stories of the frame with respect to a stationary point of reference as well as the relative displacements of the damper with respect to the second floor of the frame.

The data generated during a shaking episode was stored in the same DEC PDP 11-34 computer that is used to drive the shaking table. Signals from the accelerograms and the displacement transducers were amplified and conditioned before they were stored. Once the data was stored in the computer, transfer functions and time histories of any combination of the quantities that were monitored could be plotted at one's convenience. During the experiment, transfer functions and/or time histories could be viewed on the screen of a Scientific Atlanta fourier spectrum analyzer and could be subsequently plotted.

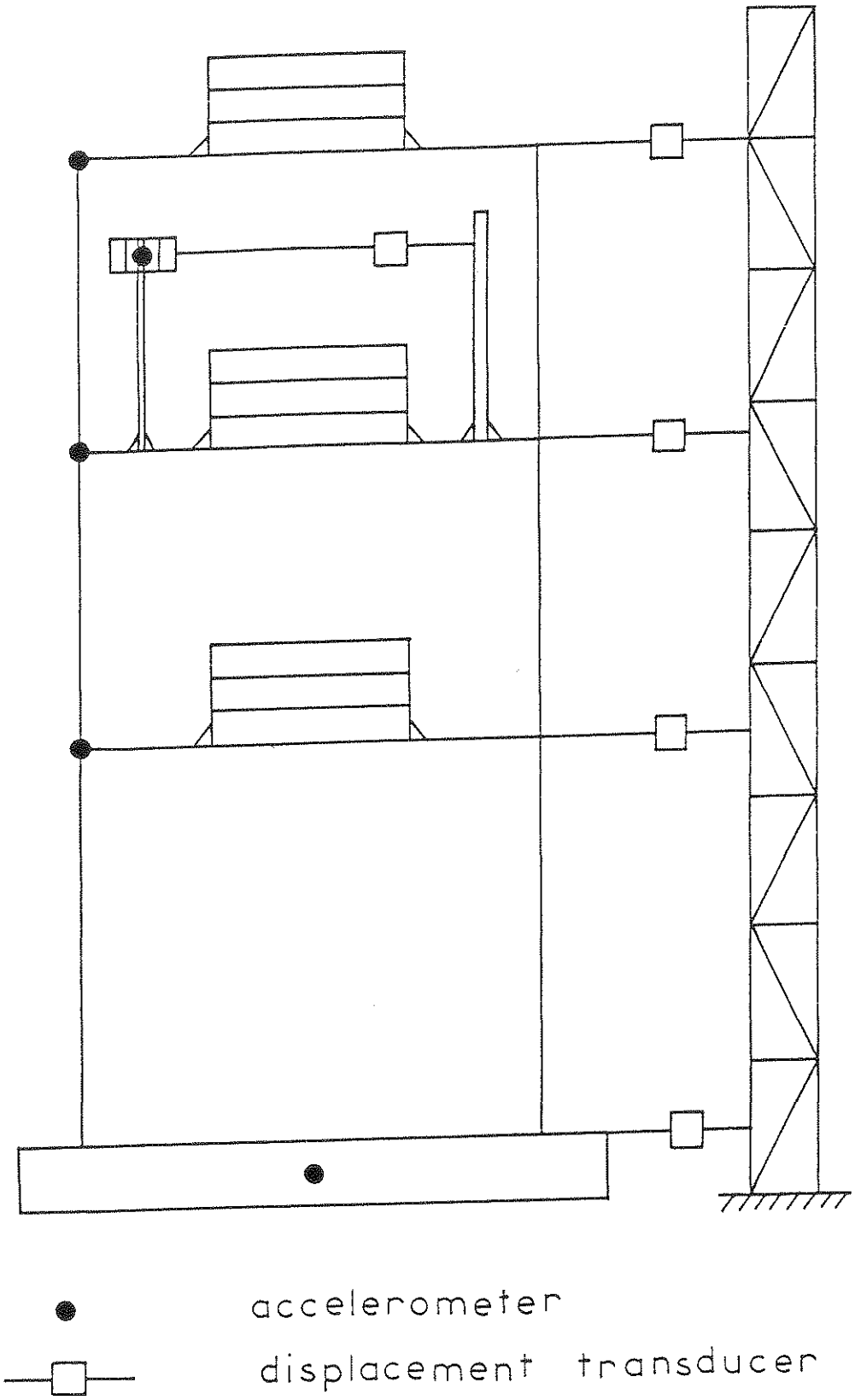

Figure 2-8 Instrumentation of the Primary-Secondary System

SECTION 3

EXPERIMENTAL RESULTS

3.1 Transfer Functions

The transfer functions are for the white noise base accelerogram and serve as a means of system identification. The following plots are included here for every coupled system case: acceleration of the damper to acceleration of the second floor of the frame (A4-A2), acceleration of damper to base acceleration (A4-AB), acceleration of the second floor of the frame to base acceleration (A2-AB), and displacement of the damper to acceleration of the second floor of the frame (D4-A2). In particular, Fig. 3-1 depicts the aforementioned plots for coupled system case 1 (frame with damper BT), Fig. 3-2 is for coupled system case 2 (frame with damper BU), Fig. 3-3 is for coupled system case 3 (frame with damper C) and Fig. 3-4 is for coupled system case 4 (frame with damper E).

3.2 Time Histories

Time histories were generated for the El Centro 1940 N-S base accelerogram. For every coupled system, the important plots are the relative acceleration time history of the damper with respect to the base (A4-B), the relative acceleration of the second floor of the frame with respect to the base (A2-B), the relative displacement of the damper with respect to the second floor of the frame (D4-2) and either the relative displacement of the second floor of the frame with respect to the base (D2-B) or the relative displacement of the damper with respect to the base (D4-B). As in the case of the transfer functions, these plots are obtained by processing the absolute accelerations and relative displacements measured by the instruments attached to the combined system. In particular, Figs. 3-5

through 3-8 depict the aforementioned plots for coupled cases 1-4, respectively.

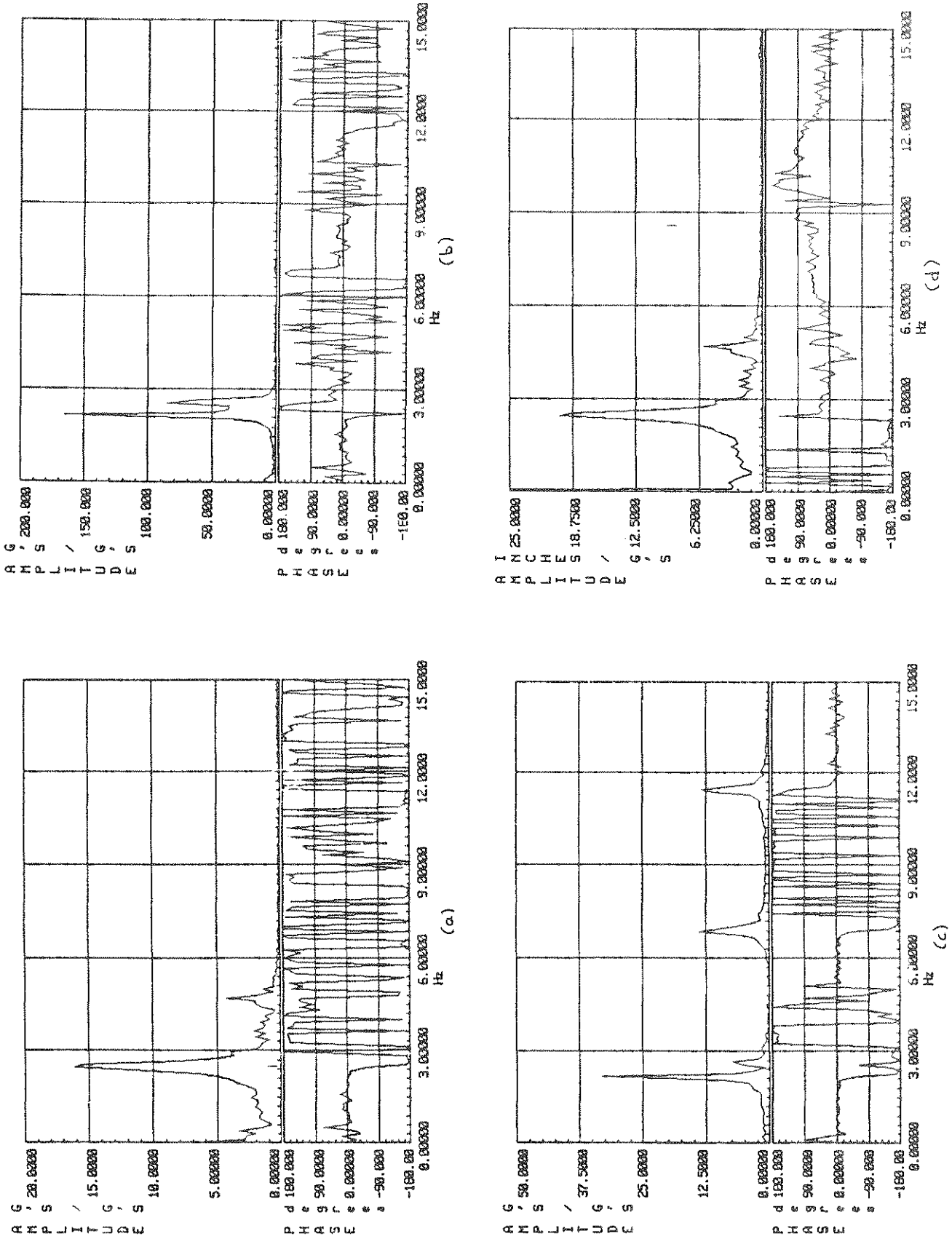

Figure 3-1 Experimentally Obtained Transfer Functions for Coupled System 1 (a) A4 to A2, (b) A4 to AB, (c) A2 to AB, (d) D4 to A2

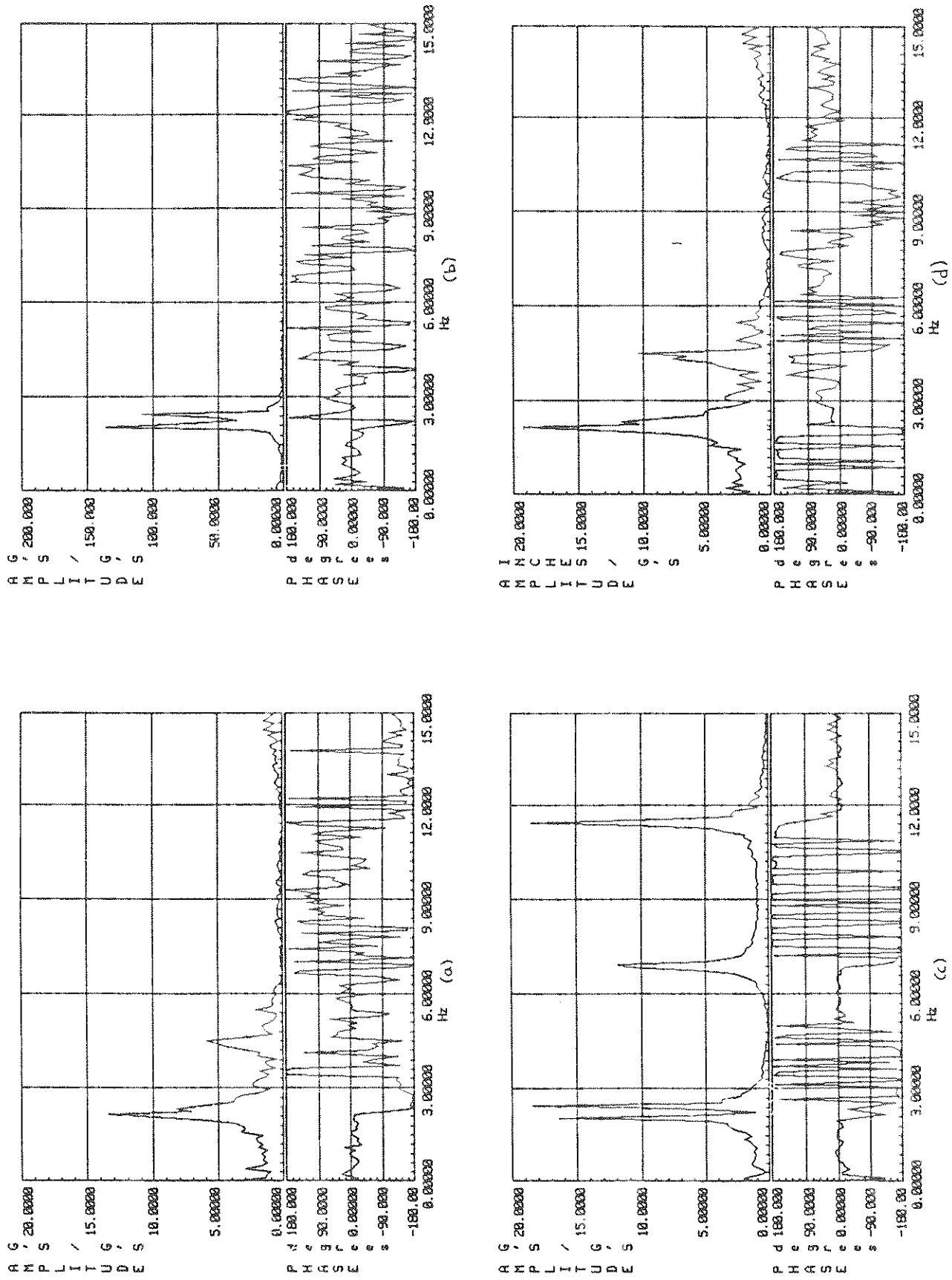

Figure 3-2 Experimentally Obtained Transfer Functions for Coupled System 2 (a) A4 to A2, (b) A4 to AB, (c) A2 to AB, (d) D4 to A2

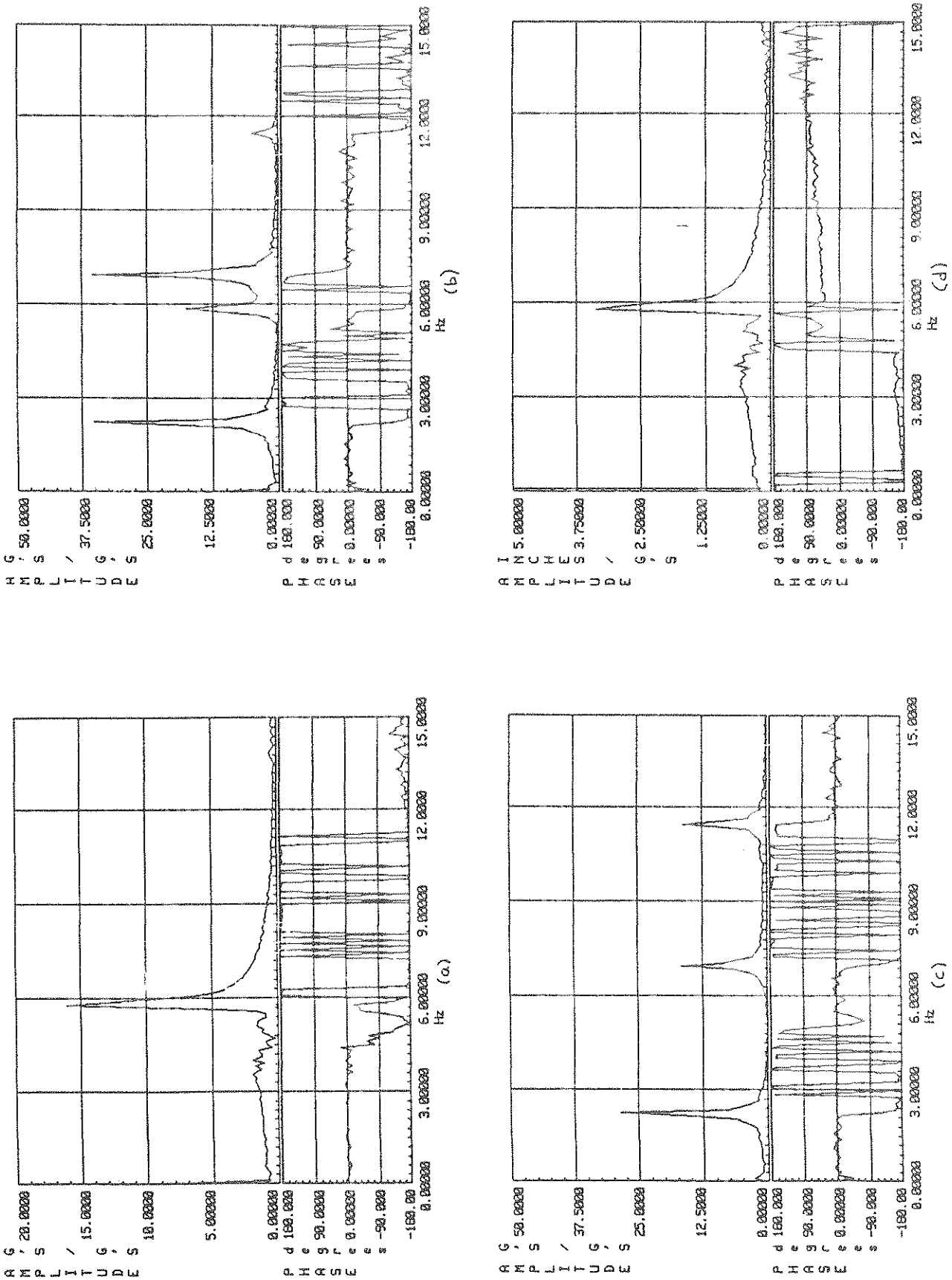

Figure 3-3 Experimentally Obtained Transfer Functions for Coupled System 3 (a) A4 to A2, (b) A4 to AB, (c) A2 to AB, (d) D4 to A2

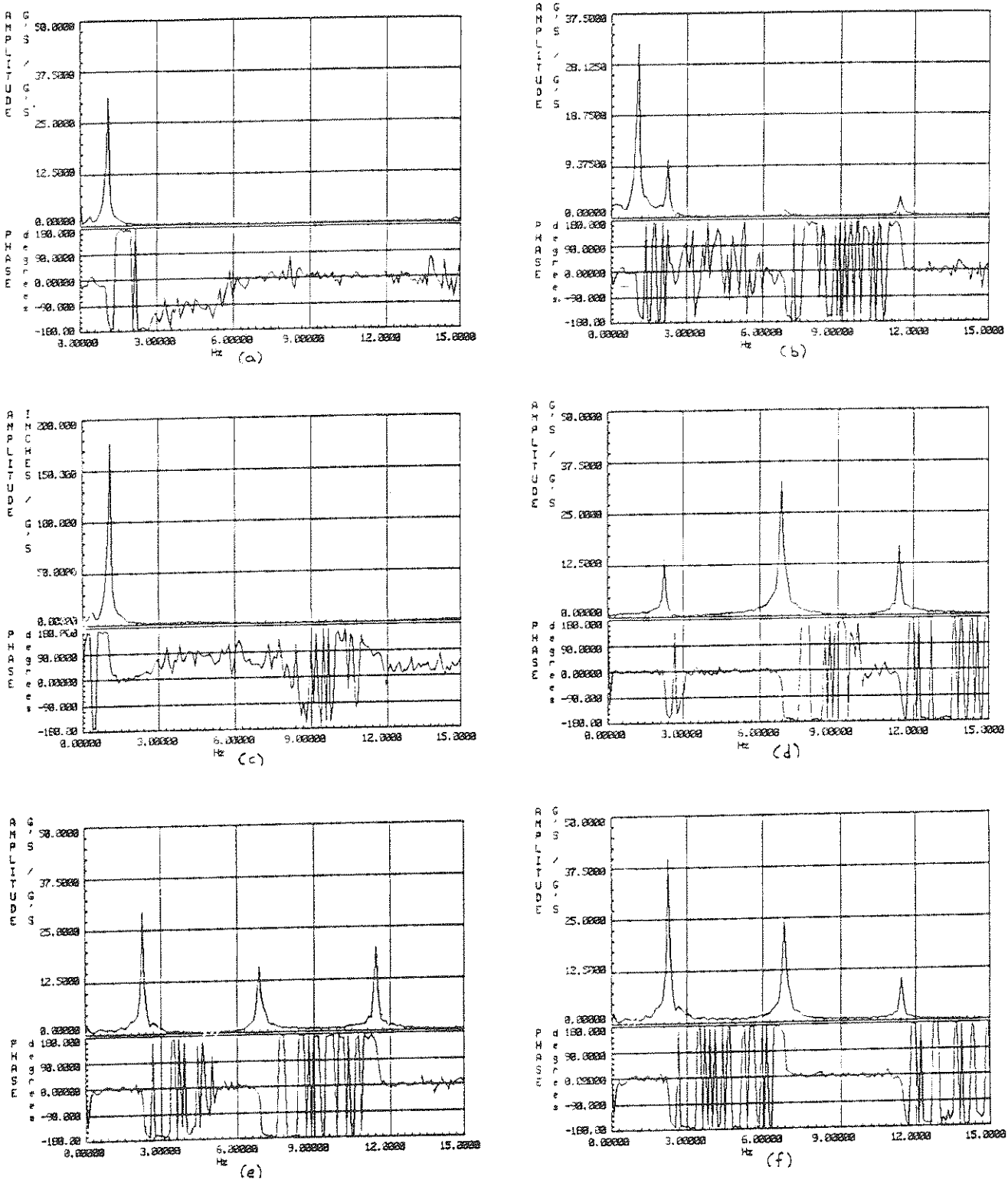

Figure 3-4 Experimentally Obtained Transfer Functions for Coupled System 4 (a) A4 to A2, (b) A4 to AB, (c) D4 to A2, (d) A1 to AB, (e) A2 to AB, (f) A3 to AB

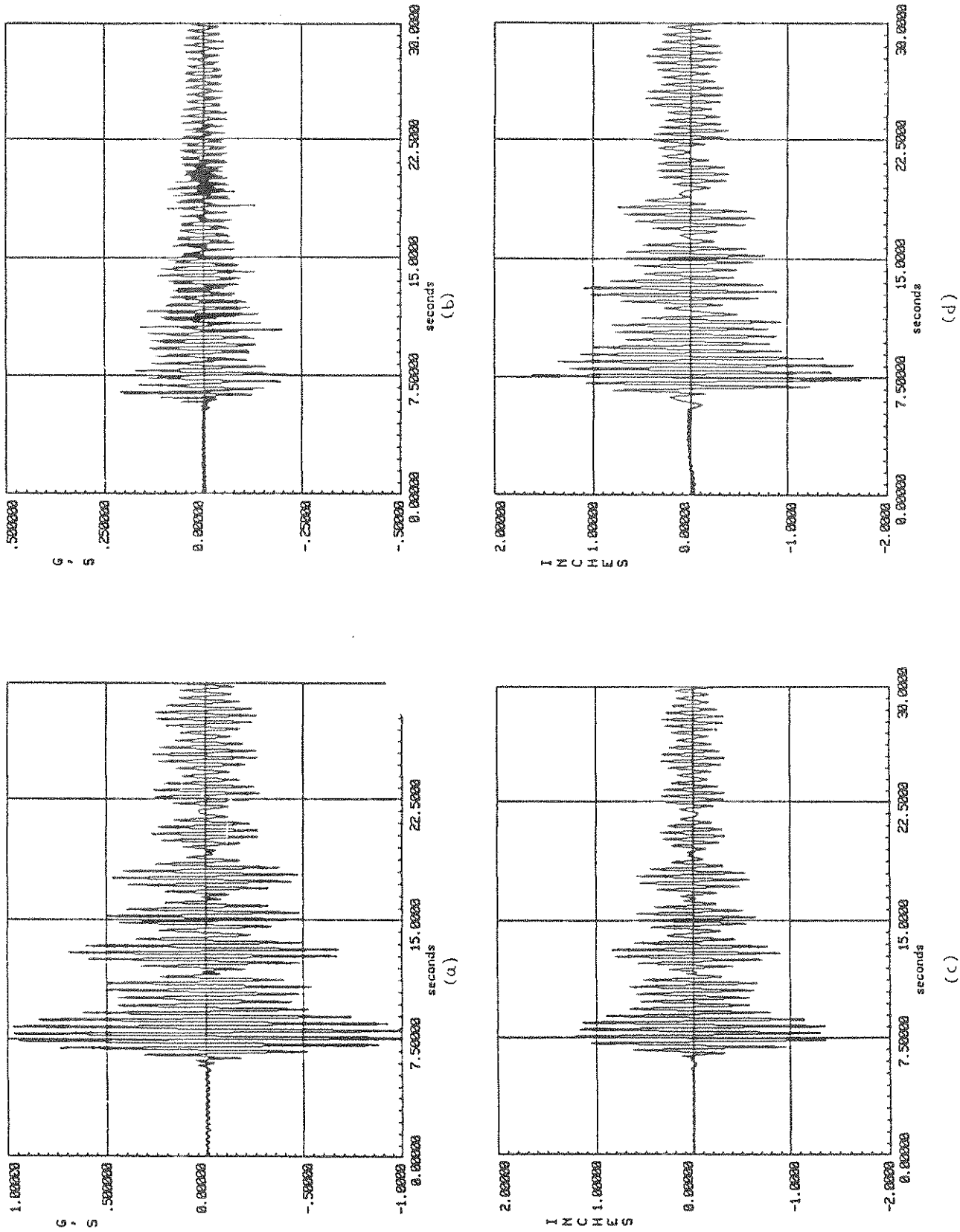

Figure 3-5 Experimentally Obtained Time Histories for Coupled Systems 1 (a) A4 to B, (b) A2 to B, (c) D4 to 2, (d) D4 to B

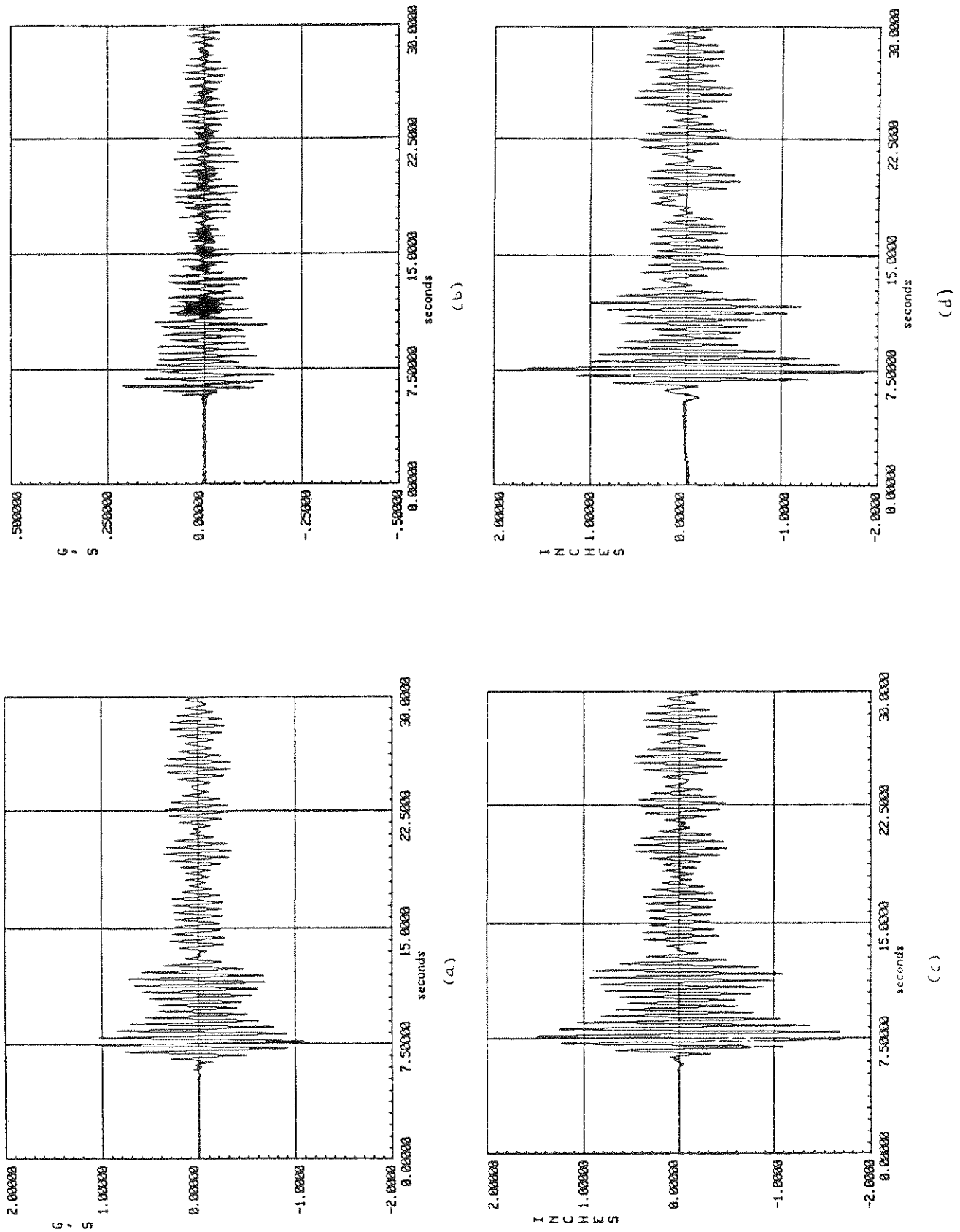

Figure 3-6 Experimentally Obtained Time Histories for Coupled System 2 (a) A4 to B, (b) A2 to B, (c) D4 to 2, (d) D4 to B

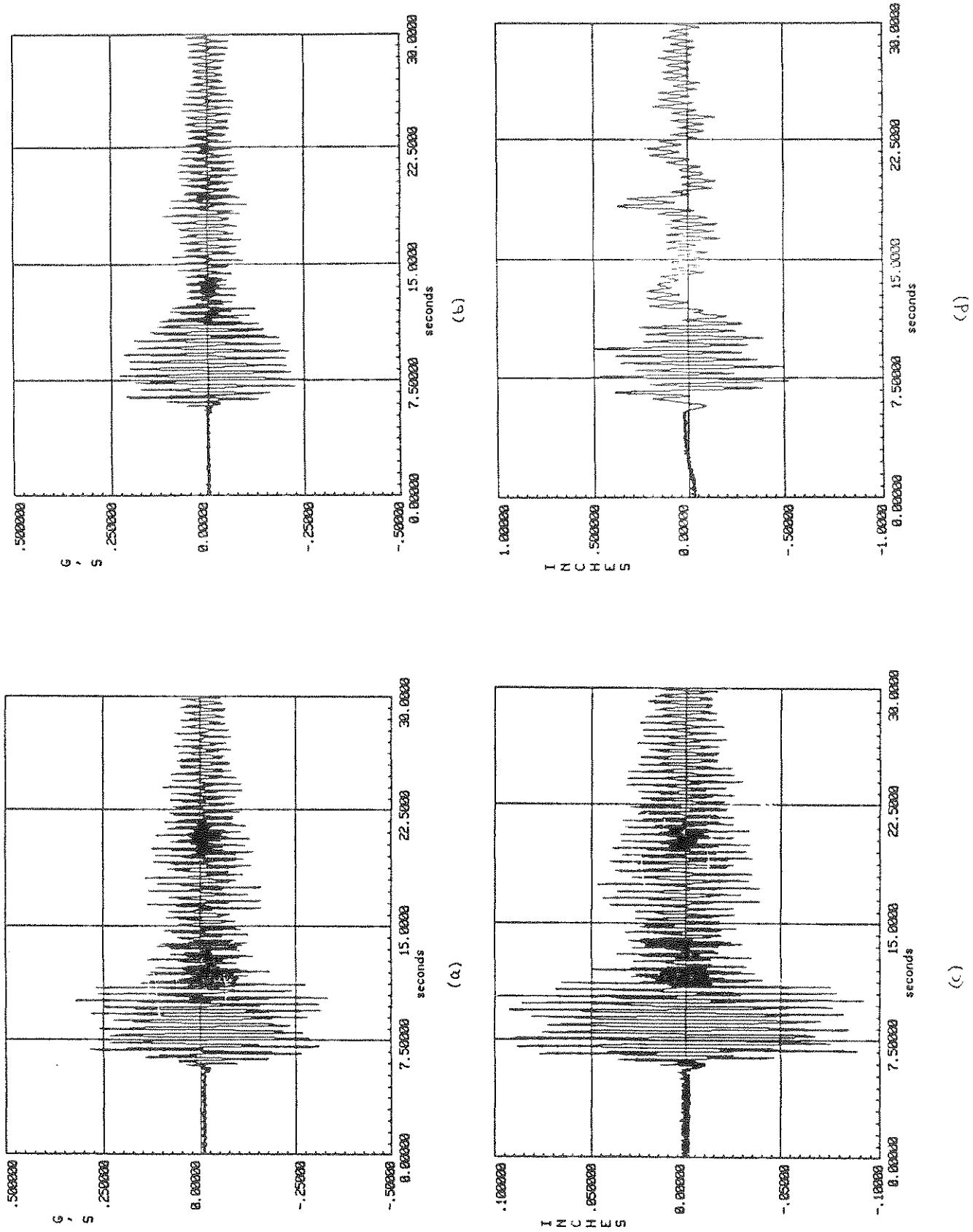

Figure 3-7 Experimentally Obtained Time Histories for Coupled System 3 (a) A4 to B, (b) A2 to B, (c) D4 to 2, (d) D2 to B

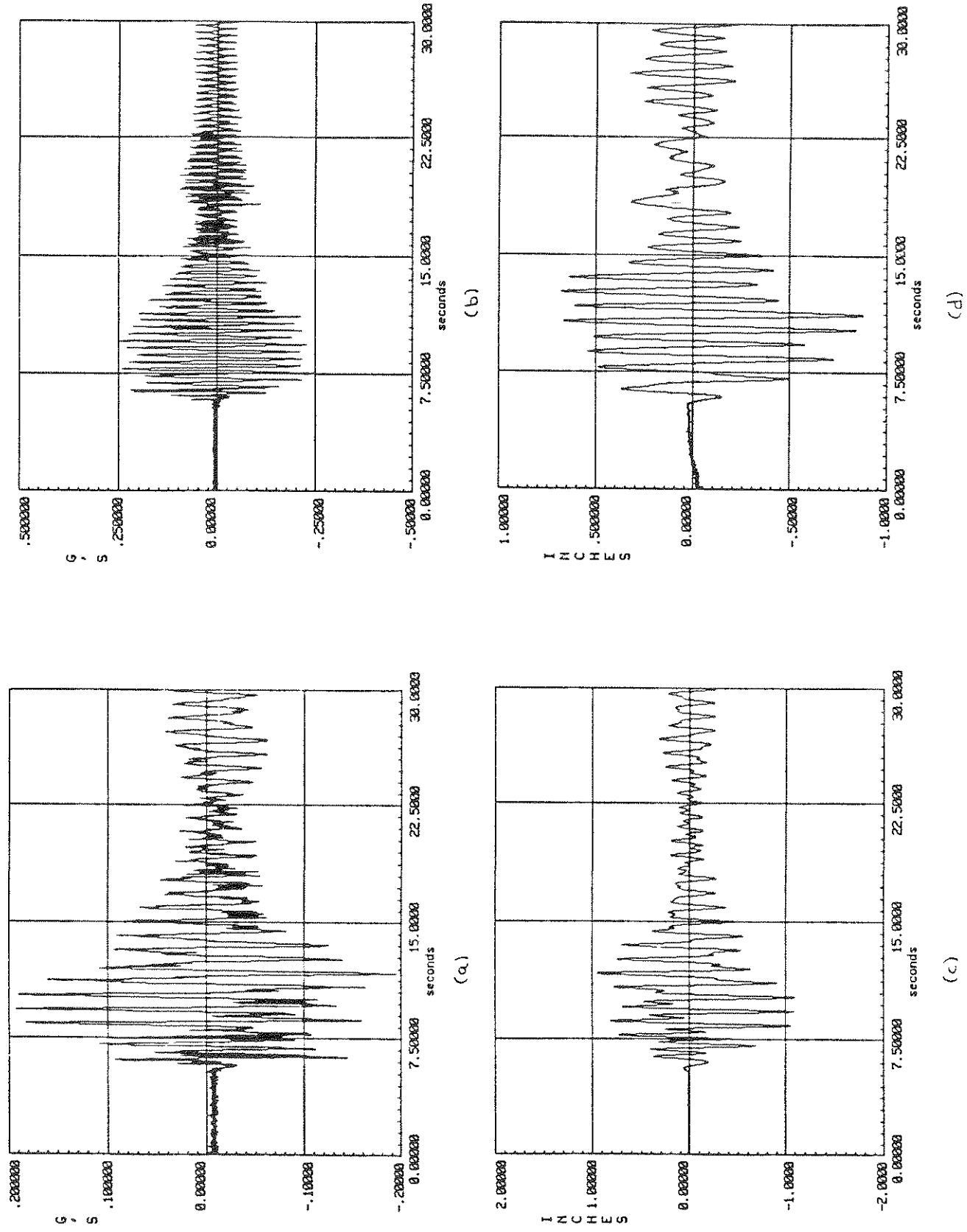

Figure 3-8 Experimentally Obtained Time Histories for Coupled System 4 (a) A4 to B, (b) A2 to B, (c) D4 to 2, (d) D4 to B

SECTION 4

INTERPRETATION OF THE EXPERIMENTAL RESULTS

4.1 Substructuring Approach

The numerical methodology used to reproduce the time histories obtained for the coupled system with the El Centro 1940 accelerogram of Fig. 2-7(b) applied at its base is a substructuring approach employing a predictor-corrector scheme especially designed to account for the interaction between the primary structure and the secondary attachments. This numerical methodology is described in detail in Manolis and Juhn (1988). One of the advantages of the methodology is that the dynamic properties of each of the constituents of the coupled system are required and not the dynamic properties of the combined system, which are more difficult to determine. The numerical methodology can work either at the physical coordinate level, in which case the mass, stiffness and damping matrices of each subsystem are required, or at the modal coordinate level, in which case the natural frequencies, modal damping ratios and modal shapes of each subsystem are required. There is an option for condensing the number of DOF of the problem by using Ritz vectors, but this is unneccesary in this case since the primary system (frame) is described by 3 DOF, while the secondary system (damper) is described by a single DOF.

At first, the results of the experimental identification process using a white noise base acceleration that are plotted in Figs. 3-1 through 3-4 for coupled system cases 1-4, respectively, are used to determine the natural frequencies, modal shapes and modal damping ratios of the frame and of the attached damper. This process is described in Section 4.2. Next,

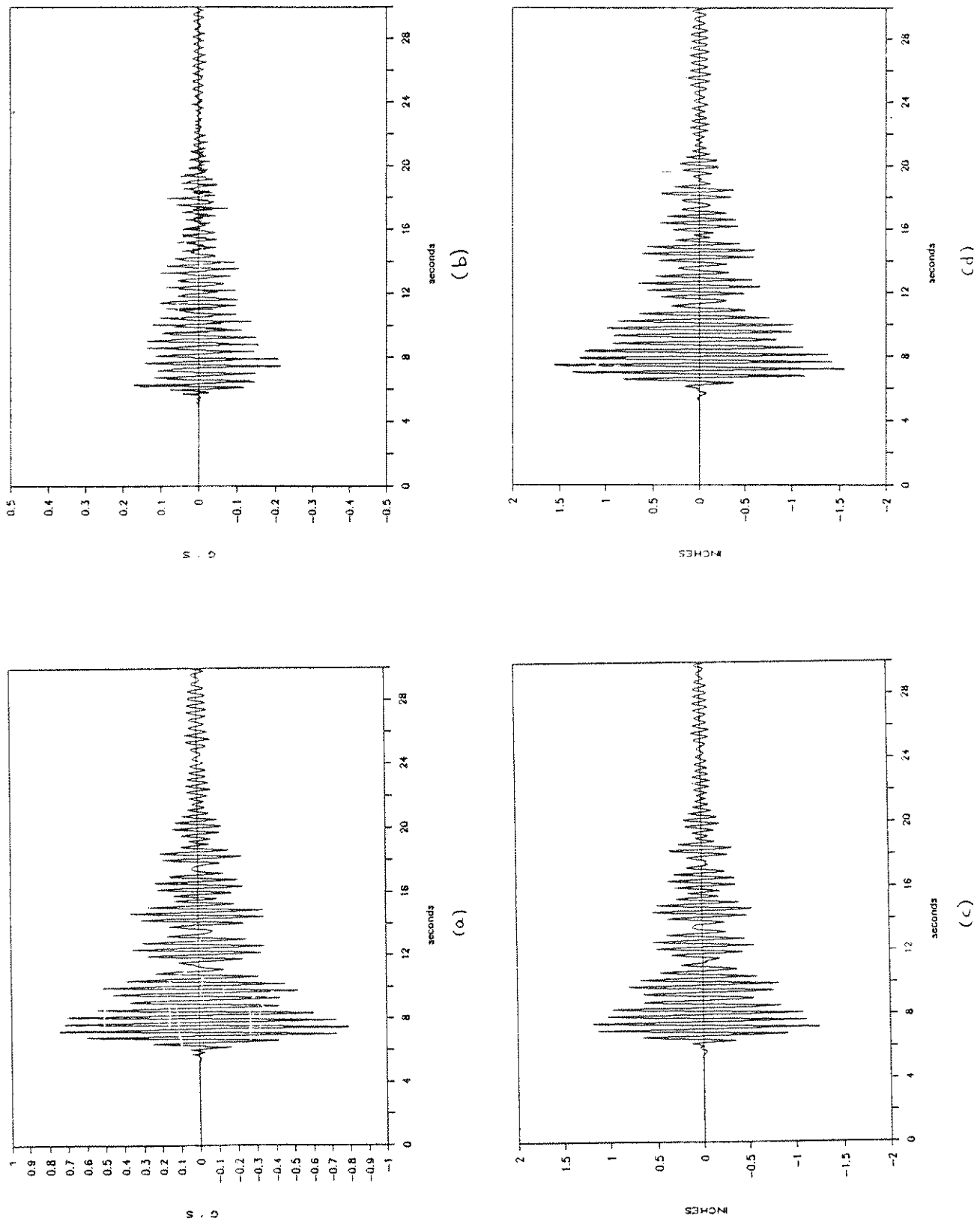

Figure 4-1 Numerically Simulated Time Histories for Coupled System 1 (a) A4 to B, (b) A2 to B, (c) D4 to 2, (d) D4 to B

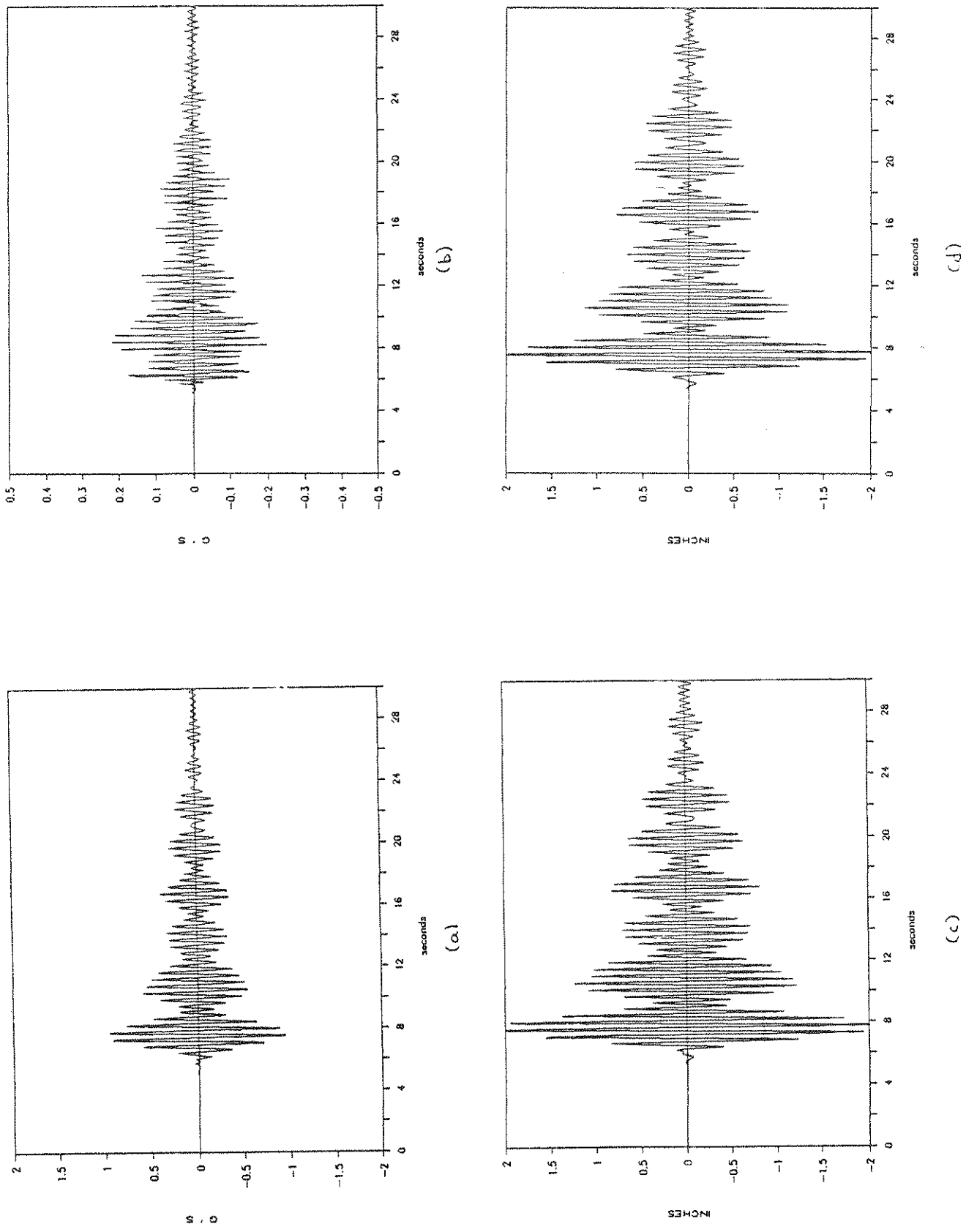

Figure 4-2 Numerically Simulated Time Histories for Coupled System 2 (a) A4 to B, (b) A2 to B, (c) D4 to 2, (d) D4 to B

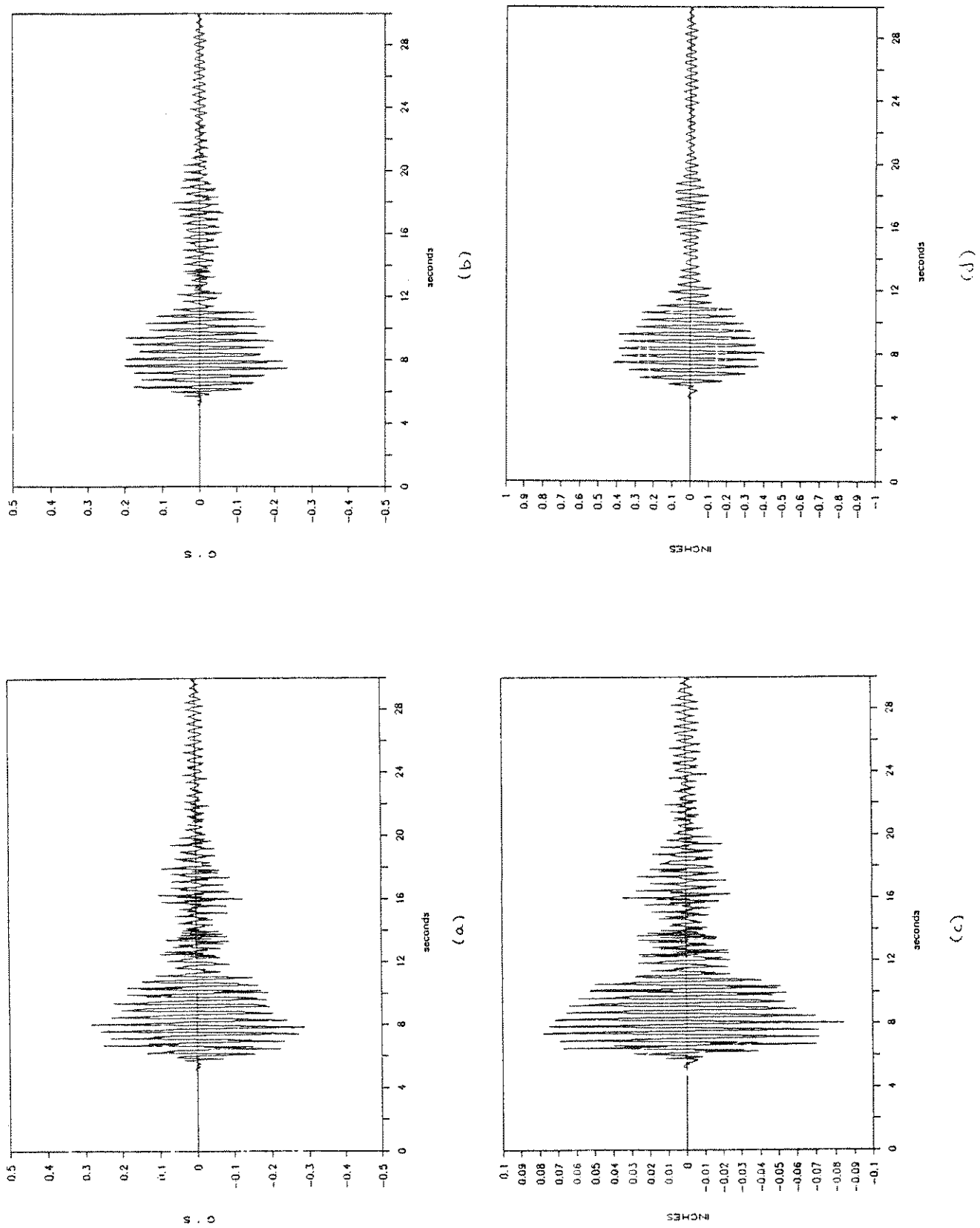

Figure 4-3 Numerically Simulated Time Histories for Coupled System 3 (a) A4 to B, (b) A2 to B, (c) D4 to 2, (d) D2 to B

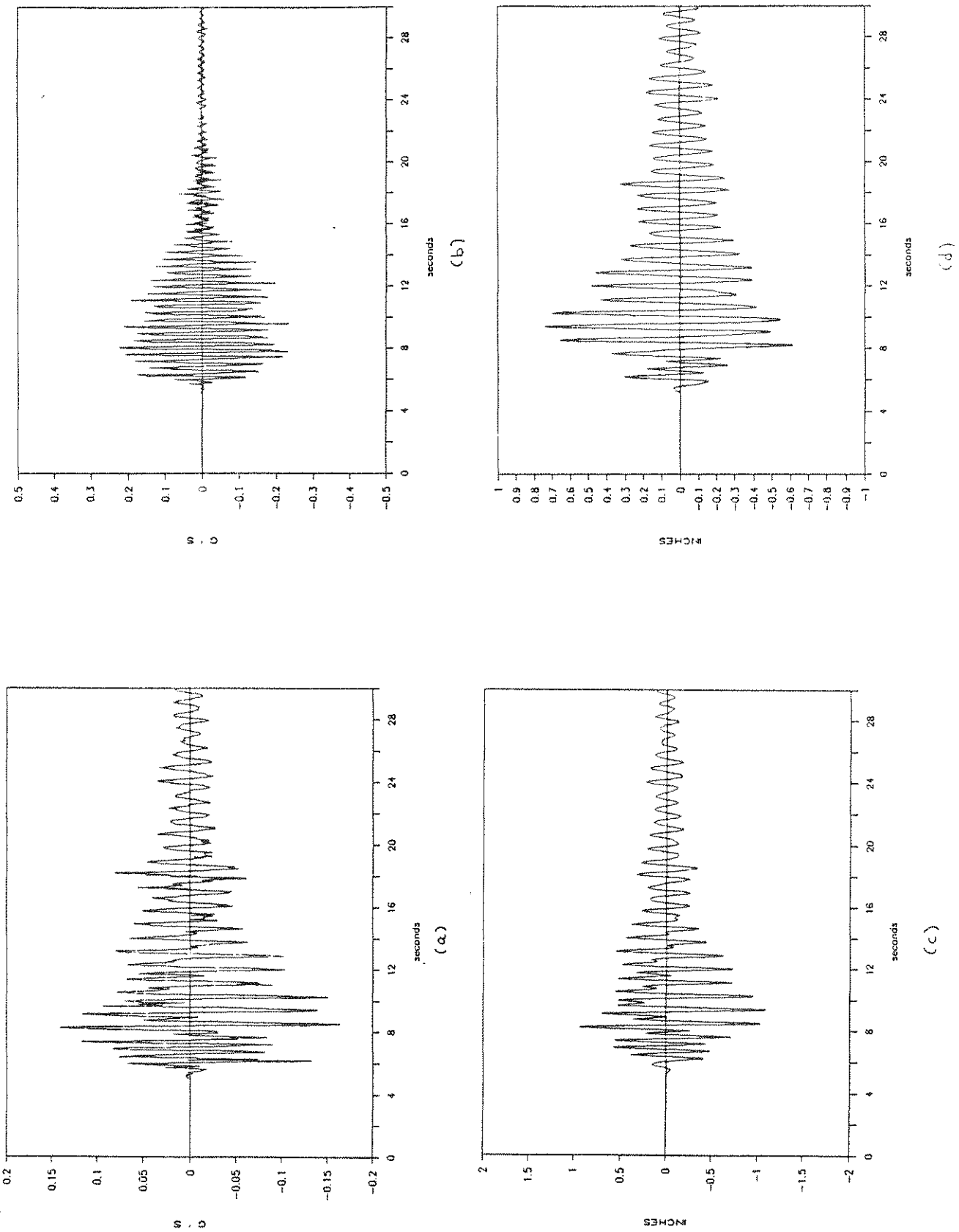

Figure 4-4 Numerically Simulated Time Histories for Coupled Systems 4 (a) A4 to B, (b) A2 to B, (c) D4 to 2, (d) D4 to B

this information is used in the substructuring approach (Manolis and Juhn 1988) whereby numerical integration is performed at the modal coordinate level. Finally, the numerical results generated (Figs. 4-1 through 4-4) for comparison with the experimentally obtained time histories (Figs. 3-5 through 3-8) are shown in Section 4.3.

4.2 Experimental Identification

The equations of motion of a lumped parameter system such as the primary structure under ground motions are of the form

$$[M]\{\ddot{x}\} + [C]\{\dot{x}\} + [K]\{x\} = -[M]\{I\}\,\ddot{x}_g \tag{4.1}$$

where [M], [C], and [K] are the mass, damping and stiffness matrices, {x(t)} are the relative displacements, {I} is the identity vector and $\ddot{x}_g(t)$ is the ground acceleration. Furthermore, dots indicate time derivatives. By introducing the transformation

$$\{x\} = [\phi]\{q\} \tag{4.2}$$

where $[\phi]$ is the matrix of eigenvectors and {q(t)} are the generalized coordinates, modal equations of the form

$$\ddot{q}_j + 2\zeta_j\omega_j\,\dot{q}_j + \omega_j^2 q_j = -\Gamma_j\ddot{x}_g \tag{4.3}$$

are obtained, where j = 1,2,...,n, n being the order of (4.1). In the above, ω_j is the jth natural frequency, ζ_j the corresponding modal damping factor, and the modal participation factor Γ_j is obtained from

$$\{\Gamma\} = [\phi]^T[M]\{I\} \;/\; ([\phi]^T[M]\{\phi\}) \tag{4.4}$$

Transforming (4.3) in the frequency domain gives

$$-\omega^2\bar{q}_j + i\omega 2\zeta_j\omega_j\bar{q}_j + \omega_j^2\bar{q}_j = -\Gamma_j\,\ddot{x}_g(\omega) \tag{4.5}$$

where the overbar denotes a Fourier transform, $i = \sqrt{-1}$ and $\ddot{x}_g(\omega)$ is the

Fourier transform of $\ddot{x}_g(t)$. Solving (4.5) for $\bar{q}_j$ gives

$$\bar{q}_j(\omega) = \frac{-\Gamma_j}{(\omega_j^2-\omega^2+2i\zeta_j\omega_j\omega)} \ddot{x}_g(\omega) \tag{4.6}$$

Reverting to physical coordinates gives

$$\bar{x}_k = \Sigma_j \phi_{kj} \bar{q}_j = - \Sigma_j \frac{\phi_{kj} \Gamma_j}{(\omega_j^2 -\omega^2+2i\zeta_j\omega_j\omega)} \ddot{x}_g(\omega) = \Sigma_j H^r_{kj}(\omega)\ddot{x}_{g(\omega)} \tag{4.7}$$

for the kth dof. $H^r_{kj}(\omega)$ is the tranfer function for the relative displacement with respect to the ground due to a ground acceleration input.

If the original equations of motion (4.1) are written for the absolute displacements

$$u_k(t) = x_k(t) + x_g(t) \tag{4.8}$$

then following along the same lines it is possible to write

$$\ddot{u}_k(\omega) = \Sigma_j \phi_{kj} \frac{\Gamma_j (2i\zeta_j\omega_j\omega+\omega_j^2)}{(\omega_j^2 -\omega^2+2i\zeta_j\omega_j\omega)} \ddot{x}_g(\omega) = \Sigma_j H^a{}_{kj}(\omega)\ddot{x}_g(\omega) \tag{4.9}$$

where $H^a_{kj}(\omega)$ is the transfer function between absolute acceleration and ground acceleration. When evaluated at a natural frequency ω_j, this transfer function becomes

$$\left| H^a_{kj}(\omega_j)\right| = \phi_{kj}\Gamma_j \frac{\sqrt{1+4\zeta_j^2}}{2\zeta_j} \tag{4.10}$$

For the sdof secondary system, where (4.1) becomes a scalarequation, we have that

$$H^r(\omega) = (\omega_s^2-\omega^2 + 2i\zeta_s\omega_s\omega)^{-1} \tag{4.11}$$

and

$$H^a(\omega) = - (2 i\zeta_s\omega_s\omega + \omega_s^2) H^r(\omega) \tag{4.12}$$

where ω_s and ζ_s are the natural frequency and damping ratio of the

secondary system. Furthermore,

$$\left|H^r(\omega_s)\right| = (2\zeta_s\omega_s^2)^{-1} \tag{4.13}$$

and

$$\left|H^a(\omega_s)\right| = \sqrt{1+4\zeta_s^2} \,/\, 2\zeta_s \tag{4.14}$$

Examples

The primary structure (frame) properties can be determined by recourse to Fig. 3-4, which plots transfer functions for damper E. Since damper E is very light (mass ratio of 1/100) and detuned, the absolute acceleration of the second floor to the base acceleration (A2-AB), Fig. 3-4(e), is the transfer function $\Sigma_j H^a_{2j}(\omega)$. The natural frequencies of the frame (in hertz) are the ordinates of the three peaks in Fig. 3-4(e). Since the natural frequencies are well spaced, the dimensionless magnitudes of the three peaks form the second row of the modal matrix $[\phi]$. A positive angle indicates that the corresponding modal shape component is positive and a negative phase angle indicates a negative component. The modal matrix is completed and the natural frequencies checked by considering transfer functions $\Sigma_j H^a_{1k}(\omega)$ and $\Sigma_j H^a_3 j(\omega)$, the absolute accelerations of the first and third floor to the base acceleration, respectively. These are plotted in Figs. 3-4(d) and (f), respectively.

A diagonal mass matrix [M] for the frame can be determined by lumping the known mass of the frame at the level of each of the three floors. The modal shapes can then be normalized so that

$$[\phi]^T[M][\phi] = \{I\} \tag{4.15}$$

and the modal participation factors $\{\Gamma\}$ determined using (4.4). The modal damping ratios ζ_j are determined from (4.10) using any of the rows of $[\phi]$ for ϕ_{kj} and the previously computed modal participation factors Γ_j. The transfer function H^a_{kj} plot must, of course, correspond to the row of modal

shapes that was used. For instance, if Fig. 3-4(e) is used for the transfer function H^a_{2j}, then the second row ϕ_{2j} of the modal matrix must also be used.

The stiffness matrix [K] can be computed from the relation

$$[\phi]^T[K][\phi] = [\Omega], \tag{4.16}$$

where $[\Omega]$ is a diagonal matrix containing the squares of the natural frequencies. Equation (4.16) holds true only if the modal matrix is normalized as shown in (4.15). Then, by inverting (4.16), the stiffness matrix becomes

$$[K] = ([\phi]^T)^{-1}\,[\Omega][\phi]^{-1} = [M][\phi][\Omega][\phi]^T[M] \tag{4.17}$$

in view of (4.15). Finally, the damping matrix [C] can be computed in the same ways as [K] from the relation

$$[\phi]^T[C][\phi] = [\Lambda], \tag{4.18}$$

where $[\Lambda]$ is a diagonal matrix containing $2\omega_j\zeta_j$ terms. All these results are collected in Table 2-I.

As far as the secondary system (damper) properties are concerned, it is best to look at the absolute acceleration of the damper to the absolute acceleration of the second floor (A4-A2) transfer function. In the case of damper E for instance, Fig. 3-4(a) shows the damper behaving as an uncoupled system so that the ordinate of the peak is the natural frequency ω_s in hertz. Since Fig. 3-4(a) is the absolute acceleration transfer function $H^a(\omega)$, (4.14) can be used to determine the damping ratio ζ_s from the dimensionless magnitude of the peak in that figure. The same information can be obtained by looking at the displacement of the damper to the absolute acceleration of the second floor (D4-A2), Fig. 12(c). In this case, the plot of Fig. 3-4(c) is the tranfer function $H^r(\omega)$ and (4.13) can be used to determine ζ_s. It should be noted, however, that when Fig. 3-4(b) showing the transfer function of the absolute acceleration of the damper to the base

acceleration is considered, then the presence of four peaks at frequencies ω_s, ω_1, ω_2, and ω_3 reveals the interaction between the primary and secondary systems.

In general, it is difficult to accurately evaluate the damping ratio ζ_s because it is very low. It was found that an average value of ζ_s of 0.01 best reproduces the peaks in Figs. 3-4(a) through (c). It should be noted that the subsequenct computations for the time histories are not that sensitive to small variations in already low damping values. In the case of used except that one has to be careful because the $H^a(\omega)$ and $H^r(\omega)$ transfer functions show spurious smaller peaks. Also, transfer functions such as A4-BA and A2-BA clearly demonstrate the interplay between the damper and the first mode of the frame to which it is tuned.

Finally, the mass m_s of a damper is easily measured so that the stiffness of the damper is found from the definition of the natural frequency, i.e., $k_s = \omega_s^2 m_s$. Also, the dampers damping coefficient $c_s = 2\zeta_s\omega_s$. All these results are collected is Table 2-II.

4.3 Numerical Simulations

Figures 4-1 through 4-4 plot the following time histories for coupled system cases 1-4, respectively: (a) relative acceleration of the damper with respect to the base (A4-B); (b) relative acceleration of the second floor of the frame with respect to the base (A2-B); (c) relative displacement of the damper with respect to the second floor of the frame, (D4-2) and (d) relative displacement of the second floor of the frame with respect to the base (D2-B) or relative displacement of the damper with respect to the base (D4-B). As mentioned previously, a time stepping technique with

substructuring capability was used (Manolis and Juhn 1988). The time step Δt was around 0.01s, which is about 10% of the first natural frequency of the combined system. Comparing these results with the experimentally obtained ones plotted in Figs. 3-5 through 3-8 for coupled system cases 1-4, respectively, the following conclusions can be drawn:

(1) In general, the numerical simulations reproduce the experimental results with a very good degree of accuracy. Note that the polarity of the accelerograms was reversed, which results in an inversion of the plots in Figs. 3-5 through 3-8. It should be kept in mind that only 4 DOF were used to represent the coupled system.

(2) The greatest difficulty in the experimental identification process is evaluation of damping.

(3) It is difficult to achieve exact tuning between primary and secondary systems in the experiment, in view of the slight variation of the individual system properties from one shaking episode to the other.

(4) Cases 1 and 2 (dampers BT and BU, respectively were nearly tuned, while cases 3 and 4 (dampers C and E, resepectively) were detuned. Due to the very low mass ratio of damper E in case 4, the primary structure does not feel the presence of the secondary system. Full fledged interaction is manifested in cases 1 and 2. Finally, despite the fact damper C is tuned, case 3 demonstrates the effect of a non-negligible secondary system on the primary structure.

(5) In general, the numerically simulated primary system (frame) response was very close to the experimentally obtained results. As far as the secondary system (damper) response is concerned, the acceleration is generally underestimated and the displacement is generally overestimated by the numerical simulations by a few percent.

(6) As far as the frame is concerned, the dampers act as energy absorption mechanisms that are more effective the finer the tuning of the damper is. Viewed from the damper point of view, detuning is an effective way of reducing the response of the damper.

(7) Table 4-I contrasts the maximum values obtained for the combined system between the response of the second floor with respect to the ground and the response of the damper with respect to the ground. This is done for both tuned (cases 1,2) and detuned (cases 3,4) situations.

TABLE 4-I

Maximum Response of Combined System

CASES	1, 2	3	4
Relative acceleration of second floor wrt the base (in g)	0.14	0.25	0.25
Relative displacement of second floor wrt the base (in inches)	0.25	0.50	0.42
Relative acceleration of damper wrt the base (in g)	1.0	0.3	0.2
Relative displacement of damper wrt the base (in inches)	2.0	0.6	0.8

SECTION 5

CONCLUSIONS

This report presented the results of a series of experiments investigating primary-secondary system interaction. A three-story, one-quarter scaled frame was used to model the primary structure and a cantilevered damper was used to represent the secondary system. The experiments were conducted on an earthquake simulator and two horizontal ground motions were considered: white noise and the El Centrol 1940, N-S accelerogram.

Experimental results were collected for both tuned and detuned situations and for a range of mass ratios of the primary to the secondary system. It was shown that it is possible to accurately reproduce the experimentally obtained time histories using numerical integration techniques within the concept of substructuring. To this purpose, properties of the primary and the secondary systems must be separately identified using experimentally obtained data. Despite some difficulties associated with system identification, the accuracy level obtained from the numerical simulations is very satisfactory.

In order to fully investigate primary-secondary system interaction, a new series of experiments is planned involving more realistic models. In particular, a scaled six-story frame that is very flexible compared to the model used herein will be used. More than one multi-DOF dampers will be attached to various locations of the frame. Also, the frame strong axis will be at an angle with respect to the direction of ground motion, which will have both horizontal and vertical components.

SECTION 6

REFERENCES

1. Burdisso, R. A. and Singh, M. P. (1987) "Seismic Analysis of Multiple Supported Secondary Systems with Dynamic Interaction Effects", Earthquake Engng. Struct. Dynamics, Vol. 15, 1005-1022.
2. Chung, L. L. , Reinhorn, A. M. and Soong, T. T. (1988) "Experiments on Active Control of Seismic Structures", ASCE J. of Engng. Mech. Vol. 114, 241-256.
3. Der Kiureghian, A., Sackman, J. L., and Nour - Omid, B. (1983) "Dynamic Analysis of Light Equipment in Structures: Response to Stochastic Input", J. Engng. Mech. ASCE, Vol. 109, No. 1, 90-110.
4. HoLung, J. A. , Cai, J., and Lin, Y. K. (1987) "Frequency Response of Secondary Systems Under Seismic Excitation", NCEER Rept. 87 - 0013, Buffalo, New York.
5. Hwang, J. S., Chang, K. C. and Lee, G. C. (1987) "The System Characteristics and Performance of a Shaking Table", NCEER Report 87-0004, Buffalo, New York.
6. Kapur, K. K. and Shao, L. C. (1973) "Generation of Seismic Floor Response Spectra for Equipment Design", Proc. Speciality Conference on Structural design of Nuclear Plant Facilities, ASCE, Chicago.
7. Kelly, J. M. (1982) "The Influence of Base Isolation on the Seismic Response of Light Secondary Equipment", Report No. UCB/EERC - 81/17, University of California, Berkeley.
8. Manolis, G. D. and Juhn, G. (1988) "Substructuring Techniques in the Time Domain for Primary-Secondary Structural Systems", NCEER Report 88-0003, Buffalo, New York.

9. Sackman, J. L. and Kelly, J. M. (1979) "Seismic Analysis of Internal Equipment and Componenets in Structures", Engineering Structures, Vol. 1, 179 - 190.

10. Singhal, A., Lutes, L. D. and Spanos, P. (1988) "Iterative Seismic Analysis of Primary-Secondary Systems", NCEER Report 88-0004, Buffalo, New York.

11. Suarez, L. E. and Singh, M. P. (1987) "Perturbed Complex Eigenproperties of Classically Damped Primary Structure and Equipment Systems", J. Sound Vib., Vol. 116, No. 2, 199-219.

12. Suzuki, H., Sugi, T., Kuwahara, M. and Kaizu, N. (1987) "Studies on Aseismic Isolation Device for Electric Substation" p. 347-358 in A. S. Cakmak, Editor, Soil-Structure Interaction, Elsevier, Amsterdam.

13. Villaverde, R. (1986) "Simplified Seismic Analysis of Secondary Systems", J. of Struc. Engng.,ASCE, Vol. 112, No. 3, 588-604.

NATIONAL CENTER FOR EARTHQUAKE ENGINEERING RESEARCH
LIST OF PUBLISHED TECHNICAL REPORTS

The National Center for Earthquake Engineering Research (NCEER) publishes technical reports on a variety of subjects related to earthquake engineering written by authors funded through NCEER. These reports are available from both NCEER's Publications Department and the National Technical Information Service (NTIS). Requests for reports should be directed to the Publications Department, National Center for Earthquake Engineering Research, State University of New York at Buffalo, Red Jacket Quadrangle, Buffalo, New York 14261. Reports can also be requested through NTIS, 5285 Port Royal Road, Springfield, Virginia 22161. NTIS accession numbers are shown in parenthesis, if available.

NCEER-87-0001 "First-Year Program in Research, Education and Technology Transfer," 3/5/87, (PB88-134275/AS).

NCEER-87-0002 "Experimental Evaluation of Instantaneous Optimal Algorithms for Structural Control," by R.C. Lin, T.T. Soong and A.M. Reinhorn, 4/20/87, (PB88-134341/AS).

NCEER-87-0003 "Experimentation Using the Earthquake Simulation Facilities at University at Buffalo," by A.M. Reinhorn and R.L. Ketter, to be published.

NCEER-87-0004 "The System Characteristics and Performance of a Shaking Table," by J.S. Hwang, K.C. Chang and G.C. Lee, 6/1/87, (PB88-134259/AS).

NCEER-87-0005 "A Finite Element Formulation for Nonlinear Viscoplastic Material Using a Q Model," by O. Gyebi and G. Dasgupta, 11/2/87, (PB88-213764/AS).

NCEER-87-0006 "Symbolic Manipulation Program (SMP) - Algebraic Codes for Two and Three Dimensional Finite Element Formulations," by X. Lee and G. Dasgupta, 11/9/87, (PB88-219522/AS).

NCEER-87-0007 "Instantaneous Optimal Control Laws for Tall Buildings Under Seismic Excitations," by J.N. Yang, A. Akbarpour and P. Ghaemmaghami, 6/10/87, (PB88-134333/AS).

NCEER-87-0008 "IDARC: Inelastic Damage Analysis of Reinforced Concrete-Frame Shear-Wall Structures," by Y.J. Park, A.M. Reinhorn and S.K. Kunnath, 7/20/87, (PB88-134325/AS).

NCEER-87-0009 "Liquefaction Potential for New York State: A Preliminary Report on Sites in Manhattan and Buffalo," by M. Budhu, V. Vijayakumar, R.F. Giese and L. Baumgras, 8/31/87, (PB88-163704/AS).

NCEER-87-0010 "Vertical and Torsional Vibration of Foundations in Inhomogeneous Media," by A.S. Veletsos and K.W. Dotson, 6/1/87, (PB88-134291/AS).

NCEER-87-0011 "Seismic Probabilistic Risk Assessment and Seismic Margins Studies for Nuclear Power Plants," by Howard H.M. Hwang, 6/15/87, (PB88-134267/AS).

NCEER-87-0012 "Parametric Studies of Frequency Response of Secondary Systems Under Ground-Acceleration Excitations," by Y. Yong and Y.K. Lin, 6/10/87, (PB88-134309/AS).

NCEER-87-0013 "Frequency Response of Secondary Systems Under Seismic Excitation," by J.A. HoLung, J. Cai and Y.K. Lin, 7/31/87, (PB88-134317/AS).

NCEER-87-0014 "Modelling Earthquake Ground Motions in Seismically Active Regions Using Parametric Time Series Methods," G.W. Ellis and A.S. Cakmak, 8/25/87, (PB88-134283/AS).

NCEER-87-0015 "Detection and Assessment of Seismic Structural Damage," by E. DiPasquale and A.S. Cakmak, 8/25/87, (PB88-163712/AS).

NCEER-87-0016 "Pipeline Experiment at Parkfield, California," by J. Isenberg and E. Richardson, 9/15/87, (PB88-163720/AS).

NCEER-87-0017 "Digital Simulation of Seismic Ground Motion," by M. Shinozuka, G. Deodatis and T. Harada, 8/31/87, (PB88-155197/AS).

NCEER-87-0018 "Practical Considerations for Structural Control: System Uncertainty, System Time Delay and Truncation of Small Control Forces," J. Yang and A. Akbarpour, 8/10/87, (PB88-163738/AS).

NCEER-87-0019 "Modal Analysis of Nonclassically Damped Structural Systems Using Canonical Transformation," by J.N. Yang, S. Sarkani and F.X. Long, 9/27/87, (PB88-187851/AS).

NCEER-87-0020 "A Nonstationary Solution in Random Vibration Theory," by J.R. Red-Horse and P.D. Spanos, 11/3/87, (PB88-163746/AS).

NCEER-87-0021 "Horizontal Impedances for Radially Inhomogeneous Viscoelastic Soil Layers," by A.S. Veletsos and K.W. Dotson, 10/15/87, (PB88-150859/AS).

NCEER-87-0022 "Seismic Damage Assessment of Reinforced Concrete Members," by Y.S. Chung, C. Meyer and M. Shinozuka, 10/9/87, (PB88-150867/AS).

NCEER-87-0023 "Active Structural Control in Civil Engineering," by T.T. Soong, 11/11/87, (PB88-187778/AS).

NCEER-87-0024 "Vertical and Torsional Impedances for Radially Inhomogeneous Viscoelastic Soil Layers," by K.W. Dotson and A.S. Veletsos, 12/87, (PB88-187786/AS).

NCEER-87-0025 "Proceedings from the Symposium on Seismic Hazards, Ground Motions, Soil-Liquefaction and Engineering Practice in Eastern North America, October 20-22, 1987, edited by K.H. Jacob, 12/87, (PB88-188115/AS).

NCEER-87-0026 "Report on the Whittier-Narrows, California, Earthquake of October 1, 1987," by J. Pantelic and A. Reinhorn, 11/87, (PB88-187752/AS).

NCEER-87-0027 "Design of a Modular Program for Transient Nonlinear Analysis of Large 3-D Building Structures," by S. Srivastav and J.F. Abel, 12/30/87, (PB88-187950/AS).

NCEER-87-0028 "Second-Year Program in Research, Education and Technology Transfer," 3/8/88, (PB88-219480/AS).

NCEER-88-0001 "Workshop on Seismic Computer Analysis and Design of Buildings With Interactive Graphics," by J.F. Abel and C.H. Conley, 1/18/88, (PB88-187760/AS).

NCEER-88-0002 "Optimal Control of Nonlinear Flexible Structures," J.N. Yang, F.X. Long and D. Wong, 1/22/88, (PB88-213772/AS).

NCEER-88-0003 "Substructuring Techniques in the Time Domain for Primary-Secondary Structural Systems," by G. D. Manolis and G. Juhn, 2/10/88, (PB88-213780/AS).

NCEER-88-0004 "Iterative Seismic Analysis of Primary-Secondary Systems," by A. Singhal, L.D. Lutes and P. Spanos, 2/23/88, (PB88-213798/AS).

NCEER-88-0005 "Stochastic Finite Element Expansion for Random Media," P. D. Spanos and R. Ghanem, 3/14/88, (PB88-213806/AS).

NCEER-88-0006 "Combining Structural Optimization and Structural Control," F. Y. Cheng and C. P. Pantelides, 1/10/88, (PB88-213814/AS).

NCEER-88-0007 "Seismic Performance Assessment of Code-Designed Structures," H.H-M. Hwang, J-W. Jaw and H-J. Shau, 3/20/88, (PB88-219423/AS).

NCEER-88-0008 "Reliability Analysis of Code-Designed Structures Under Natural Hazards," H.H-M. Hwang, H. Ushiba and M. Shinozuka, 2/29/88.

NCEER-88-0009 "Seismic Fragility Analysis of Shear Wall Structures," J-W Jaw and H.H-M. Hwang, 4/30/88.

NCEER-88-0010 "Base Isolation of a Multi-Story Building Under a Harmonic Ground Motion - A Comparison of Performances of Various Systems," F-G Fan, G. Ahmadi and I.G. Tadjbakhsh, 5/18/88.

NCEER-88-0011 "Seismic Floor Response Spectra for a Combined System by Green's Functions," F.M. Lavelle, L.A. Bergman and P.D. Spanos, 5/1/88.

NCEER-88-0012 "A New Solution Technique for Randomly Excited Hysteretic Structures," G.Q. Cai and Y.K. Lin, 5/16/88.

NCEER-88-0013 "A Study of Radiation Damping and Soil-Structure Interaction Effects in the Centrifuge," K. Weissman, supervised by J.H. Prevost, 5/24/88, to be published.

NCEER-88-0014 "Parameter Identification and Implementation of a Kinematic Plasticity Model for Frictional Soils," J.H. Prevost and D.V. Griffiths, to be published.

NCEER-88-0015 "Two- and Three-Dimensional Dynamic Finite Element Analyses of the Long Valley Dam," D.V. Griffiths and J.H. Prevost, 6/17/88, to be published.

NCEER-88-0016 "Damage Assessment of Reinforced Concrete Structures in Eastern United States," A.M. Reinhorn, M.J. Seidel, S.K. Kunnath and Y.J. Park, 6/15/88.

NCEER-88-0017 "Dynamic Compliance of Vertically Loaded Strip Foundations in Multilayered Viscoelastic Soils," S. Ahmad and A.S.M. Israil, 6/17/88.

NCEER-88-0018 "An Experimental Study of Seismic Structural Response With Added Viscoelastic Dampers," R.C. Lin, Z. Liang, T.T. Soong and R.H. Zhang, 6/30/88.

NCEER-88-0019 "Experimental Investigation of Primary - Secondary System Interaction," G.D. Manolis, G. Juhn and A.M. Reinhorn, 5/27/88.

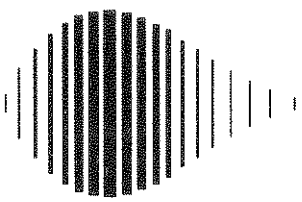

National Center for Earthquake Engineering Research
State University of New York at Buffalo